Quarterly Report Massachusetts Institute of Technology **GAGE Facility GPS Data Analysis Center Coordinator**

Thomas Herring and Mike Floyd

Period: 2025/07/01-2025/09/30

Table of Contents

| Summary | 2 |
|--|-----|
| GPS Analysis of Level 2a and 2b products | |
| Level 2a products: Rapid products | |
| Level 2a products: Final products | |
| Level 2a products: 12-week, 26-week supplement products | |
| Analysis of Final products: June 15, 2025–September 27, 2025 | |
| Table 1: Statistics of the fits of 2007 stations for CWU analyzed in the finals | |
| Table 2: Head and tail of WRMS scatter summary file CWU_FIN_Y7Q1.tab | 5 |
| GLOBK Apriori coordinate file and earthquake files | .12 |
| Snapshot velocity field analysis from the reprocessed PBO analysis | .13 |
| Table 3: Statistics of the fits of 2756 stations analyzed CWU in the reprocessed | .13 |
| Earthquake Analyses: 2025/03/15-2025/09/15 | .20 |
| Antenna and other discontinuity events. | |
| Anomalous sites | |
| GNSS Rapid processing | .26 |
| Table 4: Mean differences between GPS-only and GPS+Galileo rapid solutions | |
| ANET Processing | .27 |
| Table 5: Statistics of the fits of 34 stations in the ANET region | 28 |
| References | |

Summary

Under the GAGE2 Facility Data Analysis sub-award, MIT has been processing SINEX files from Central Washington University (CWU) and aligning them to the GAGE NAM14 reference frame. In this report, we show analyses of the data processing for the period 2025/07/01 to 2025/09/30, as well as time series velocity field analyses for the GAGE processing (1996-2025). Several earthquakes were investigated this quarter up to 2025/09/15, and two of them generated detectable co-seismic offsets. These events were EQ77 ANSS(ComCat) us7000qd1y mww7.3 Sand Point, Alaska; date and time 2025/07/16 20:38, and A5 was added as Q78 ANSS(ComCat) us6000qw60 mww8.8 Kamchatka Peninsula; Date and time 2025/07/29 23:25.

Analysis files (pbo format velocity files and offset files) are generated monthly and sent via Python in the middle of each month.

We continue to process ANET data. These solutions are in the ANT14 frame as defined in the ITRF2014 plate motion model [*Altamimi et al.*, 2017].

GPS Analysis of Level 2a and 2b products

Level 2a products: Rapid products

Final and rapid level 2a products have been, in general, generated routinely during this quarter for the CWU solutions. The description of these products, the delivery schedule, and the delivery list remain unchanged from the previous quarter and will not be reported here.

Level 2a products: Final products

The final products are generated weekly and are based on the final JPL orbits and clocks. Finals and rapid solutions are now being generated in the IGS14 system. In this quarter, 2007 stations were processed, 5 more than last quarter. In addition, up to 34 sites were processed in the ANET solutions, one less than last quarter. The number of stations processed fluctuated as data systems were updated at EarthScope.

Level 2a products: 12-week, 26-week supplement products

Each week, we also process the Supplemental (12-week latency) and six-month supplemental (26-week latency) analyses from CWU for the main GAGE2 Networks of the Americas stations (NOTA). The delivery schedule for these products is also unchanged.

Analysis of Final products: June 15, 2025–September 27, 2025

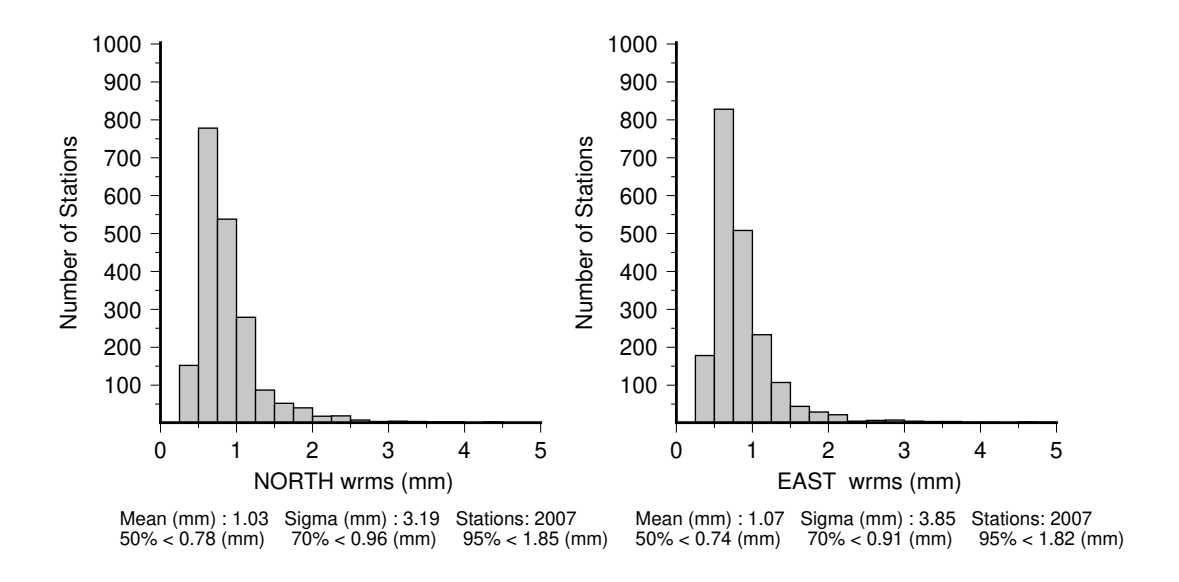
For this report, we generated the statistics using the ~3 months of CWU results between June 15, 2025, and September 27, 2025. These results are summarized in Table 1 and Figure 1.

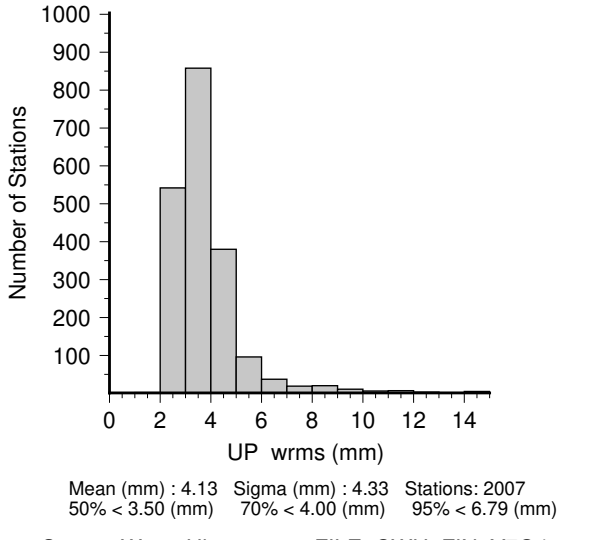
For the three months of the final position time series generated, we fit linear trends and annual signals and compute the RMS scatters of the position residuals in north, east, and up for each station in the analysis. Table 1 shows the median (50%), 70%, and 95% limits for the RMS scatters CWU. The detailed histograms of the RMS scatters are shown in Figure 1 CWU.

Table 1: Statistics of the fits of 2007 stations for CWU analyzed in the finals analysis between June 15, 2025, and September 27, 2025.

Figure 1 shows histograms of the RMS scatters.

| | 0 | | | |
|--------------|------------|-----------|---------|--|
| Center | North (mm) | East (mm) | Up (mm) | |
| Median (50%) | | | | |
| CWU | 0.78 | 0.74 | 3.50 | |
| 70% | | | | |
| CWU | 0.96 | 0.91 | 4.00 | |
| 95% | | | | |
| CWU | 1.85 | 1.82 | 6.79 | |





Scatter-Wrms Histogram : FILE: CWU_FIN_Y7Q4.sum

Figure 1: CWU solution histograms of the North, East, and Up RMS scatters of the position residuals for 2007 stations analyzed between June 15, 2025 and September 27, 2025. Linear trends and annual signals were estimated from the time series.

For the CWU analysis, we also evaluate the RMS scatters of the position estimates by network type. The figures below are based on our monthly submissions, but here, we use nominally three months of data to evaluate the RMS scatters. In Table 2, we give the median, 70, and 95 percentile limits on the RMS scatters. The geographical distributions of the RMS scatters by network type are shown in Figures 2-7. The values plotted are given in

CWU FIN Y7Q4.tab. There are 2007 stations in the file for sites with at least two measurements during the month.

Table 2: Head and tail of WRMS scatter summary file CWU_FIN_Y7Q1.tab. Tabular Position RMS scatters created from CWU_FIN_Y7Q4.sum ChiN/E/U are square root of chisquared degree of freedom of the fits. Values of ChiN/E/U near unity indicate that the estimated error bars are consistent the scatter of the position estimates

| .Site | # | N (mm) | ChiN | E (mm) | ChiE | U (mm) | ChiU | Years |
|-------|-----|--------|------|--------|------|--------|------|-------|
| 1LSU | 105 | 1.4 | 0.79 | 1.8 | 0.90 | 6.5 | 0.76 | 22.43 |
| 1NSU | 105 | 1.0 | 0.67 | 1.1 | 0.71 | 3.8 | 0.60 | 21.69 |
| 1ULM | 105 | 0.9 | 0.64 | 1.1 | 0.75 | 4.0 | 0.66 | 22.29 |
| 70DM | 105 | 0.7 | 0.42 | 0.6 | 0.44 | 3.4 | 0.52 | 24.44 |
| ••• | | | | | | | | |
| ZDV1 | 75 | 0.7 | 0.42 | 0.8 | 0.59 | 3.6 | 0.62 | 22.32 |
| ZKC1 | 75 | 0.8 | 0.53 | 0.7 | 0.50 | 4.1 | 0.69 | 22.32 |
| ZLA1 | 75 | 0.7 | 0.46 | 0.8 | 0.63 | 4.1 | 0.66 | 22.32 |
| ZLC1 | 75 | 0.7 | 0.40 | 0.9 | 0.62 | 3.8 | 0.63 | 22.55 |
| ZME1 | 75 | 1.1 | 0.72 | 0.6 | 0.48 | 4.0 | 0.65 | 22.55 |
| ZMP1 | 75 | 0.7 | 0.44 | 0.7 | 0.53 | 4.8 | 0.81 | 22.79 |
| ZNY1 | 75 | 0.7 | 0.43 | 0.6 | 0.45 | 3.6 | 0.62 | 22.70 |
| ZOA1 | 75 | 0.6 | 0.39 | 0.7 | 0.56 | 2.7 | 0.47 | 23.24 |
| ZSE1 | 75 | 0.7 | 0.37 | 0.8 | 0.59 | 3.0 | 0.51 | 22.70 |
| ZTL4 | 75 | 1.3 | 0.89 | 7.1 | 1.17 | 22.9 | 0.00 | 0.00 |

Table 2: RMS scatter of the position residuals for the CWU solution between June 15, 2025, and September 27, 2025, divided by network type. The division of networks is based on the JAVA script unavcoMetdata.jar with network codes PBO, Nucleus, Mid-SCIGN_USGS, America GAMA, COCONet and Expanded **PBO**

| Network | North (mm) | East (mm) | Up (mm) | #Sites |
|------------|------------|-----------|---------|--------|
| Median | | | | |
| PBO | 0.68 | 0.66 | 3.16 | 829 |
| NUCLEUS | 0.64 | 0.64 | 3.11 | 191 |
| GAMA | 0.91 | 0.90 | 4.04 | 14 |
| COCONet | 1.29 | 1.28 | 5.08 | 73 |
| USGS_SCIGN | 0.70 | 0.70 | 3.28 | 127 |
| Expanded | 0.88 | 0.84 | 3.90 | 774 |
| 70% | | | | |
| PBO | 0.83 | 0.80 | 3.56 | |
| NUCLEUS | 0.74 | 0.72 | 3.36 | |
| GAMA | 0.93 | 0.96 | 4.11 | |

| COCONet | 1.50 | 1.55 | 5.97 | |
|------------|------|------|-------|--|
| USGS_SCIGN | 0.88 | 0.85 | 3.65 | |
| Expanded | 1.03 | 1.04 | 4.33 | |
| 95% | | | | |
| PBO | 1.66 | 1.45 | 5.40 | |
| NUCLEUS | 1.37 | 1.10 | 4.50 | |
| GAMA | 1.22 | 1.07 | 4.27 | |
| COCONet | 3.90 | 6.75 | 14.06 | |
| USGS_SCIGN | 1.58 | 1.38 | 5.58 | |
| Expanded | 2.00 | 2.04 | 7.58 | |

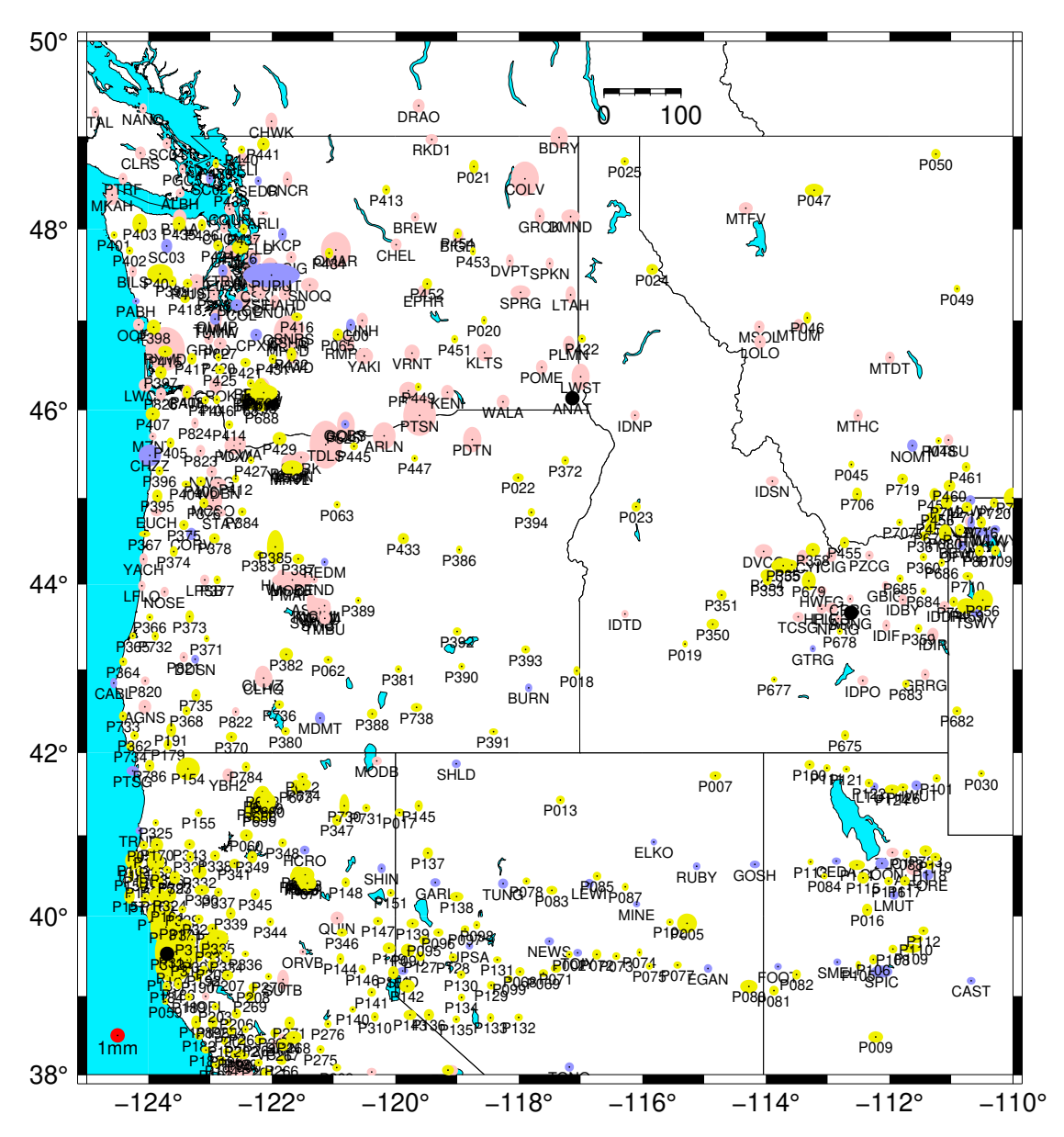


Figure 2: Distribution of the RMS scatters of horizontal position estimates from the CWU analysis for the Northern Western United States. The color of the ellipses that give the north and east RMS scatters denotes the network given by the legend in the figure. The small red circle shows the size of 1 mm scatters. Sites shown with black circles have combined RMS scatters in north and east greater than 5 mm or are sites that have no data during this 3-month interval.

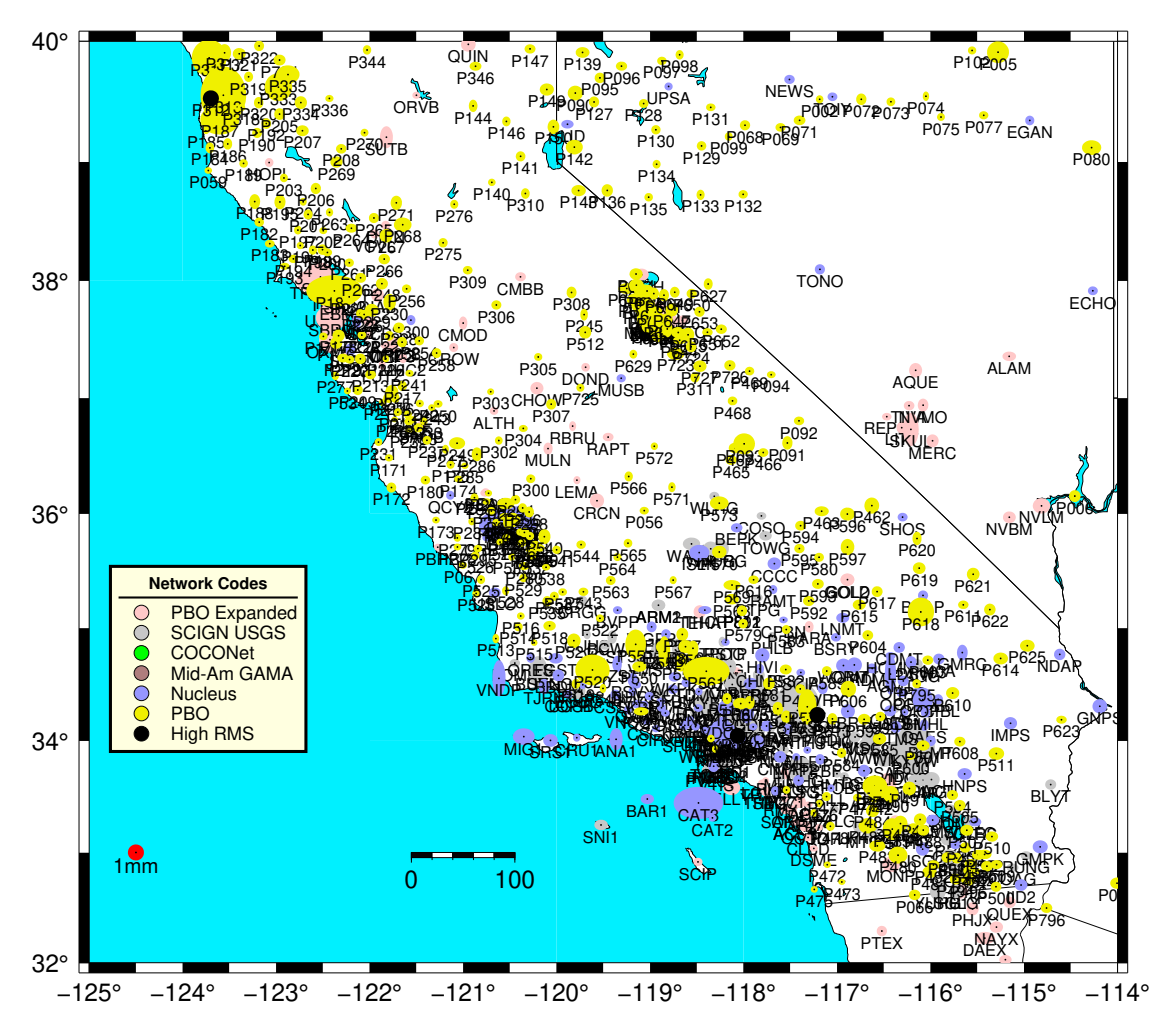


Figure 3: Same as Figure 4 except for the Southern Western United States. Black circles show large RMS scatter sites.

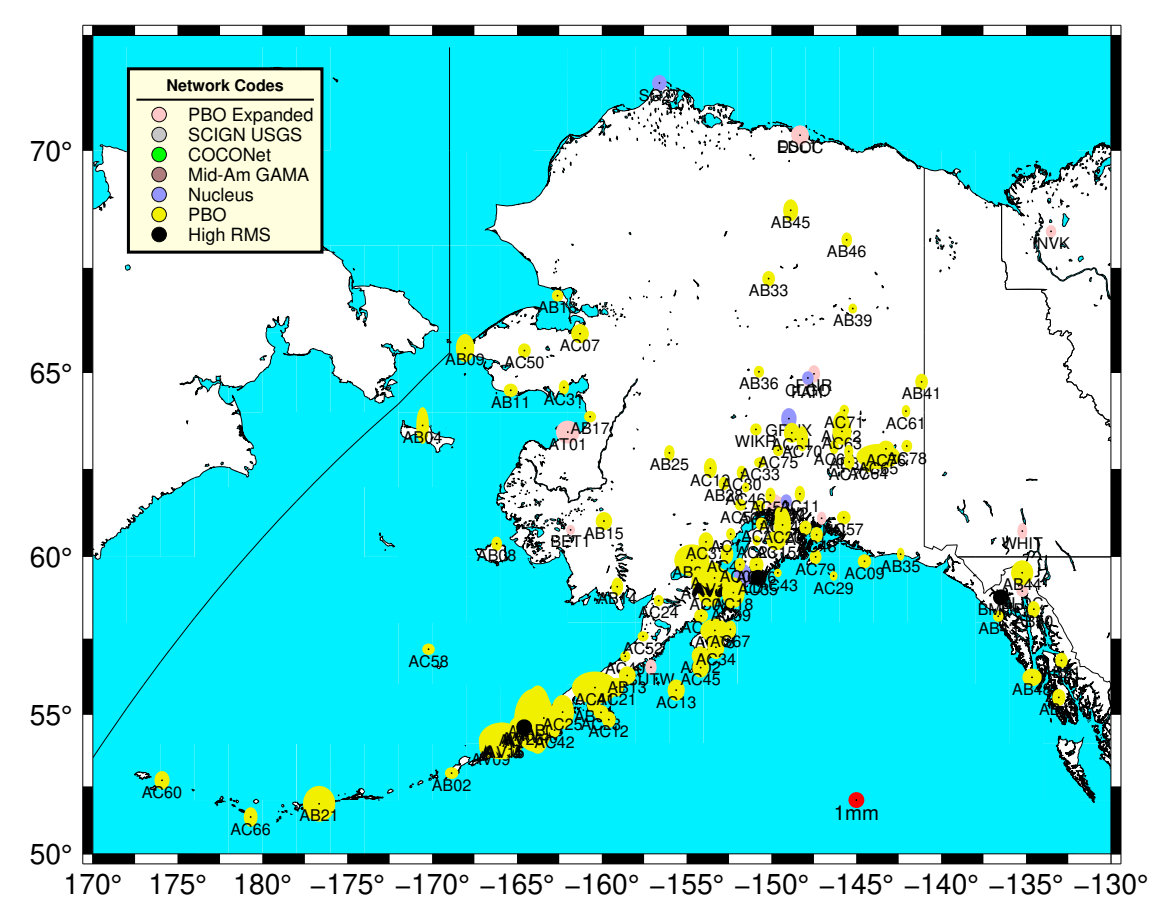


Figure 4: Same as Figure 4 except for the Alaskan region.

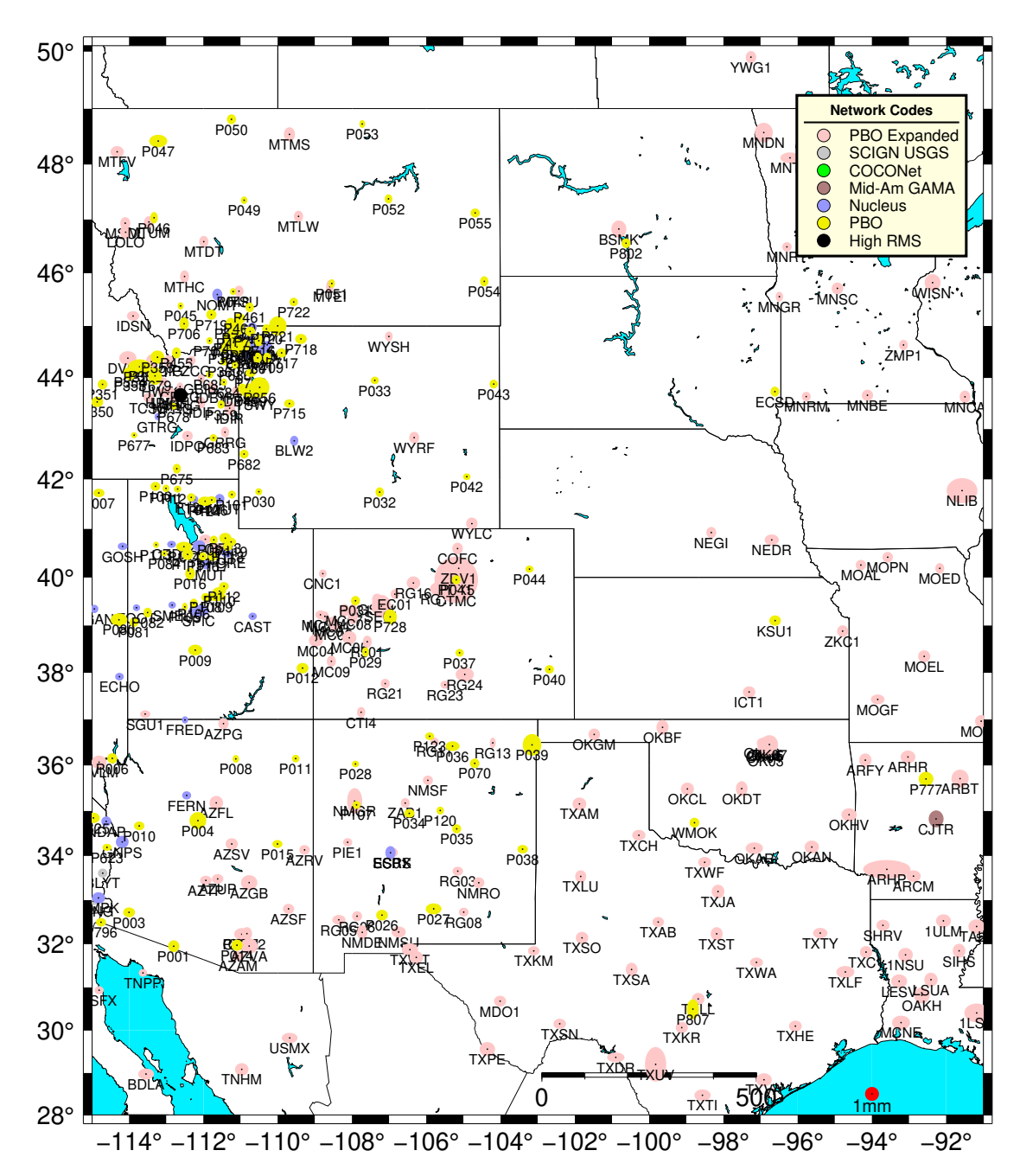


Figure 5: Same as Figure 4 except for the Central United States

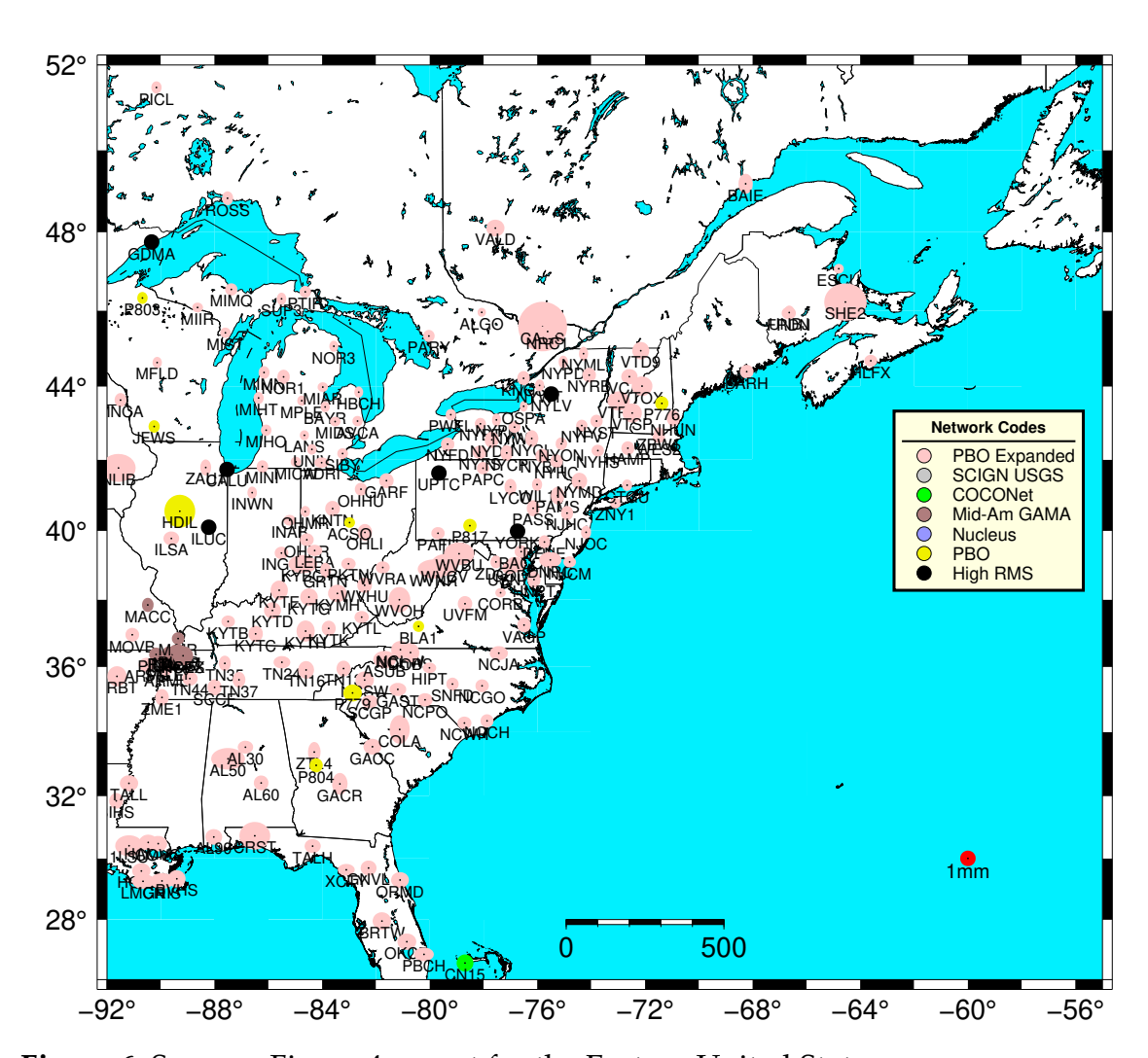


Figure 6: Same as Figure 4 except for the Eastern United States

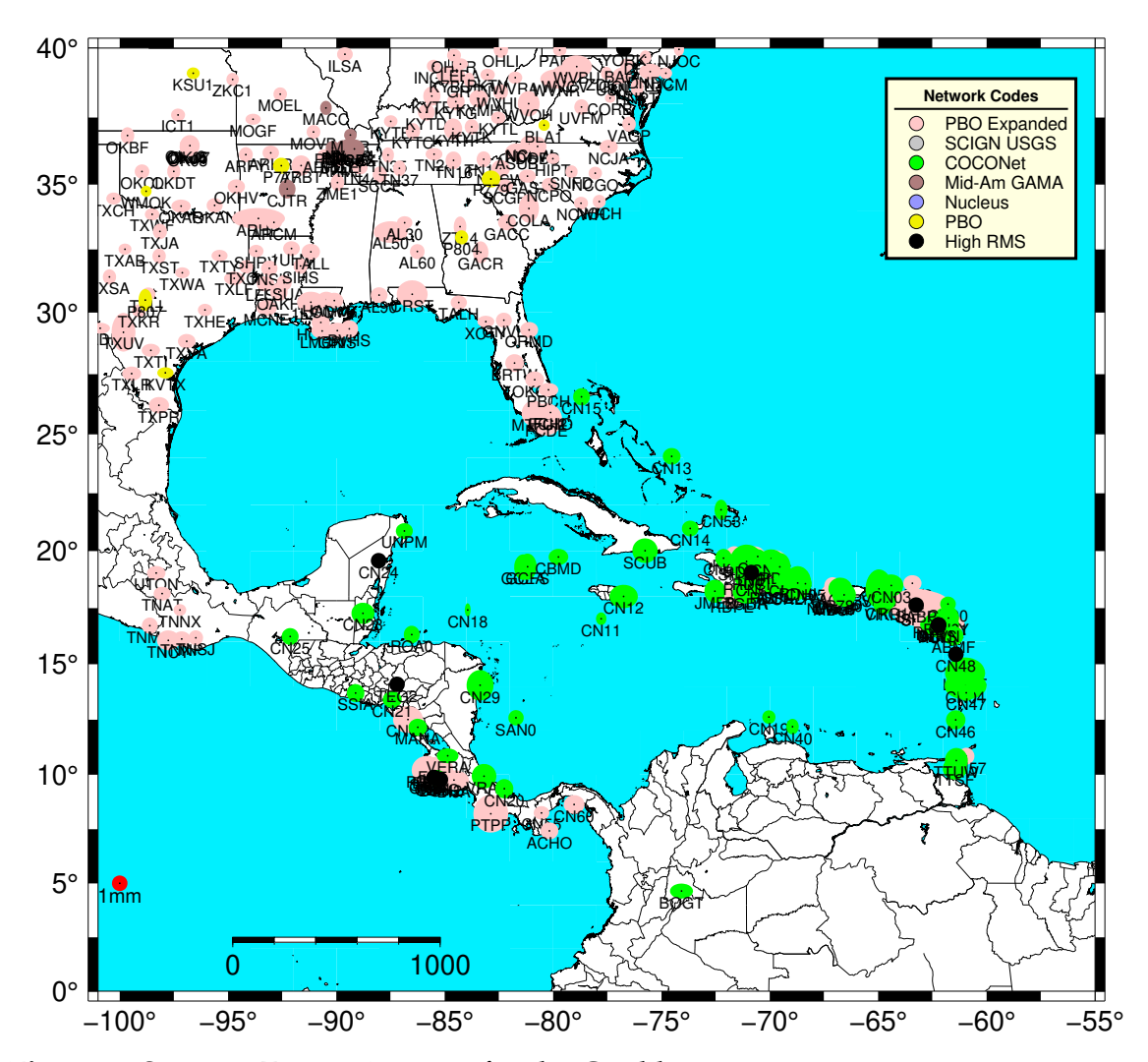


Figure 7: Same as Figure 4 except for the Caribbean region.

GLOBK Apriori coordinate file and earthquake files

As part of the quarterly analysis, we run a complete analysis of the time series files and generate position, velocity, and other parameter estimates from these time series. These files can be directly used in the GLOBK analysis files sent with the GAGE analysis documentation. The current earthquake and discontinuity files used in the GAGE ACC analyses are <u>All NOTA eqs.eq All NOTA ants.eq All NOTA unkn.eq</u>. These names have been changed to reflect that they now refer to the Network of America and no longer just the plate boundary observatory. The GLOBK apriori coordinate file <u>All CWU nam14.apr</u> is the current estimate based on data analysis in this quarterly report.

Snapshot velocity field analysis from the reprocessed PBO analysis.

For this quarterly report, we generate velocity estimates for the reprocessed results and the current GAGE analyses that are in the NAM14 reference frame using the CWU analysis. There are 2756 stations in the CWU solution. The statistics of the fits to results are shown in Table 3. Because these are cumulative statistics, they are little changed from last quarter. In this analysis, offsets are estimated for antenna changes and earthquakes. Annual signals are estimated, and for some earthquakes, logarithmic post-seismic signals are also estimated. The full tables of RMS fit, along with the duration of the data used, are given in <u>cwu nam14 250621.tab</u>. The velocity estimates are shown by region and network type in Figures 8-14. The color scheme used is the same as Figures 2-7. The snapshot velocity field file for CWU is <u>cwu_nam14_250621.snpvel</u>.

Table 3: Statistics of the fits of 2756 stations analyzed CWU in the reprocessed analysis for data collected between Jan 1, 1996 and September 27, 2025.

| Center | North (mm) | East (mm) | Up (mm) |
|--------------|------------|-----------|---------|
| Median (50%) | | | |
| CWU | 1.41 | 1.37 | 6.25 |
| 70% | | | |
| CWU | 1.78 | 1.74 | 7.12 |
| 95% | | | |
| CWU | 4.23 | 3.91 | 11.82 |

In Figures 8-14, different tolerances are used for maximum standard deviation in each figure so that regions with small velocity vectors can be displayed at large scales without the plots being dominated by large error bar points. The standard deviations of the velocity estimated are computed using the GLOBK First-order-Gauss-Markov Extrapolation (FOGMEX) model that aims to account for temporal correlations in the time series residuals. This algorithm is also called the "Realistic Sigma" model.

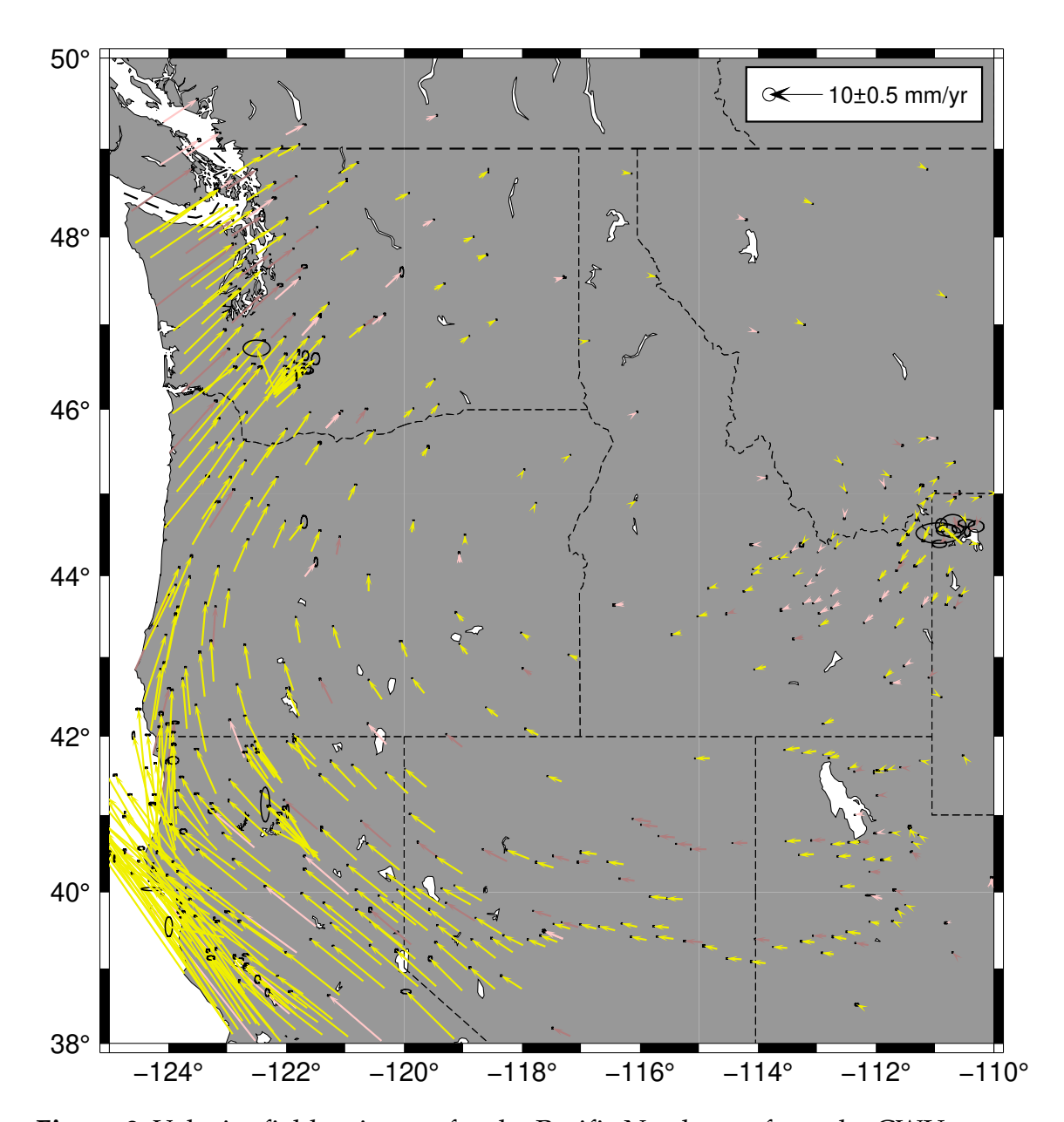


Figure 8: Velocity field estimates for the Pacific Northwest from the CWU solution generated using time series analysis and the FOGMEX error model. 95% confidence interval error ellipses are shown. The color scheme of the vectors matches the network type legend in Figure 4. Only velocities with horizontal standard deviations less than 2 mm/yr are shown (this value is reduced from previous reports due to the improved velocity sigmas).

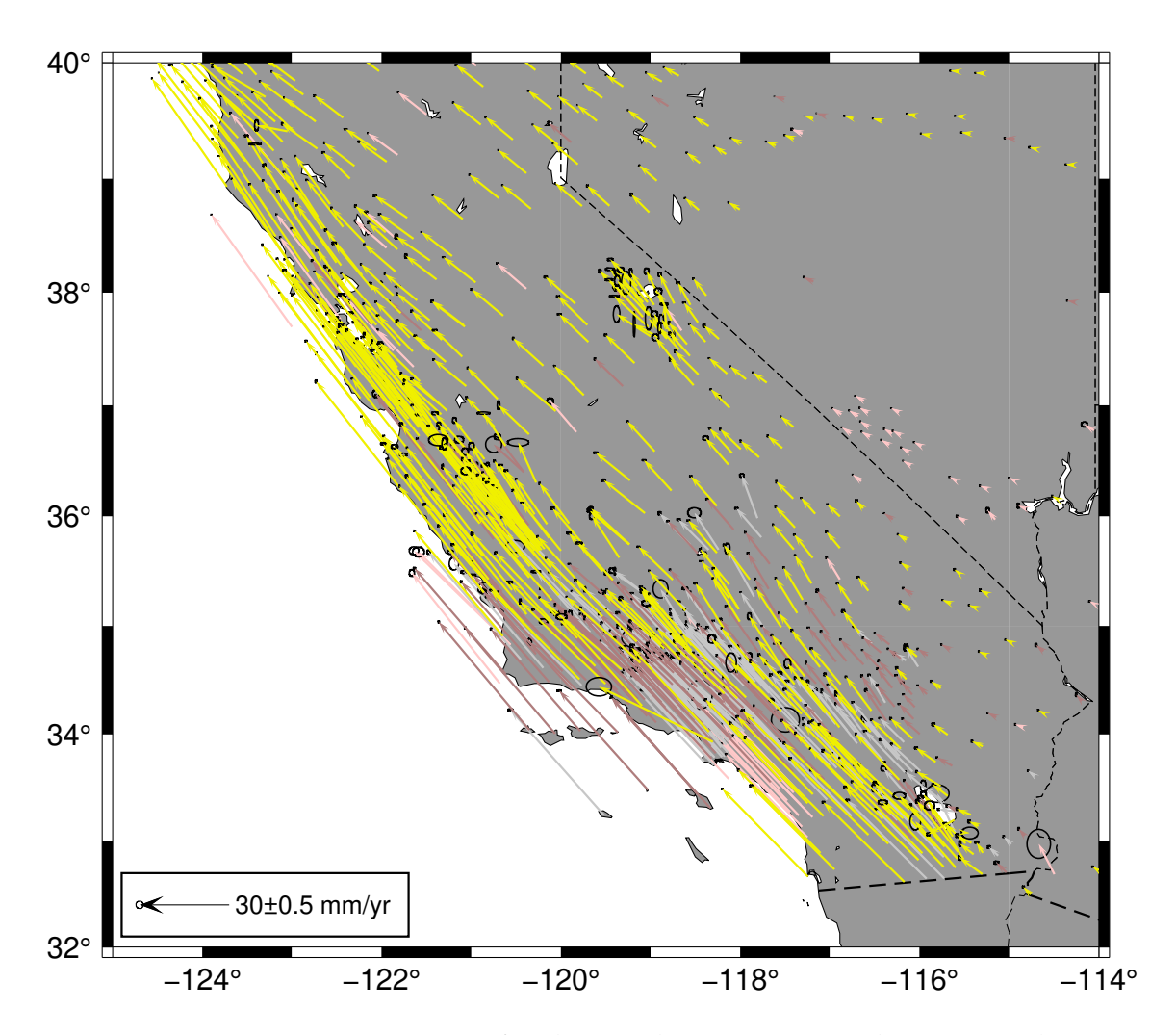


Figure 9: Same as Figure 8 except for the Southwestern United States. Only velocities with horizontal standard deviations less than 2 mm/yr are shown.

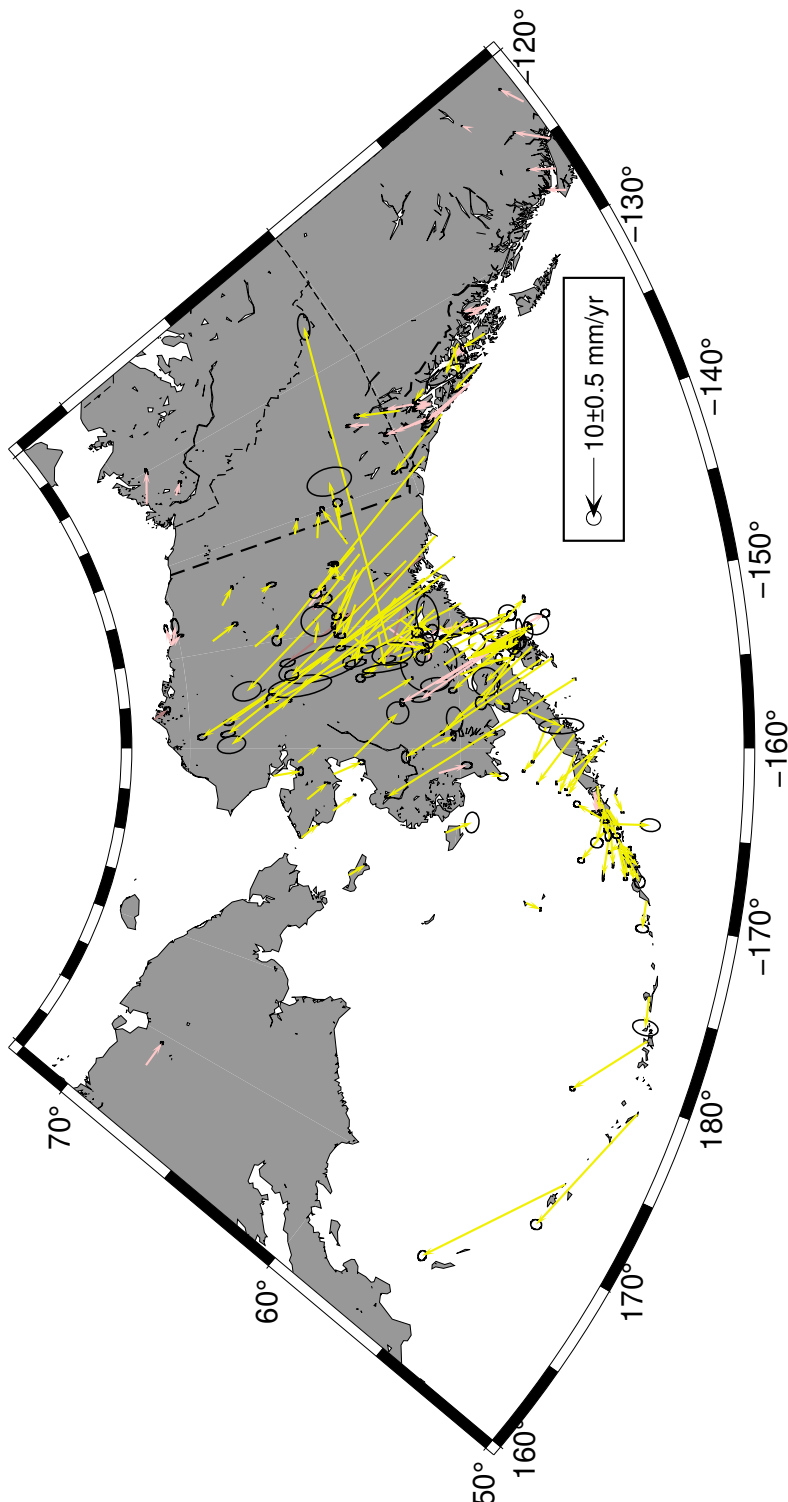


Figure 10: Same as

Figure 8 except for Alaska. Only velocities with horizontal standard deviations less than 5 mm/yr are shown

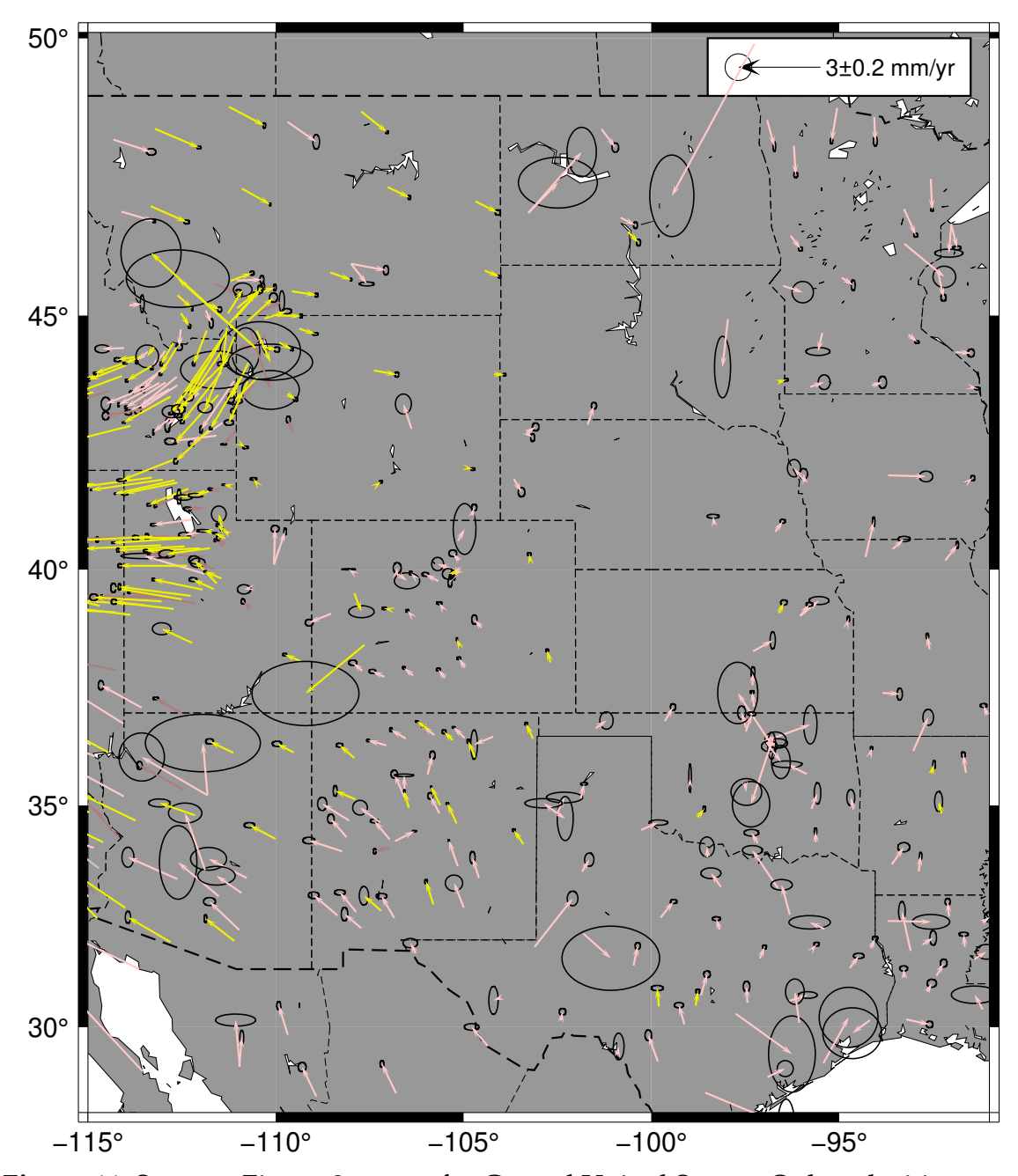


Figure 11: Same as Figure 8 except for Central United States. Only velocities with horizontal standard deviations less than 1 mm/yr are shown.

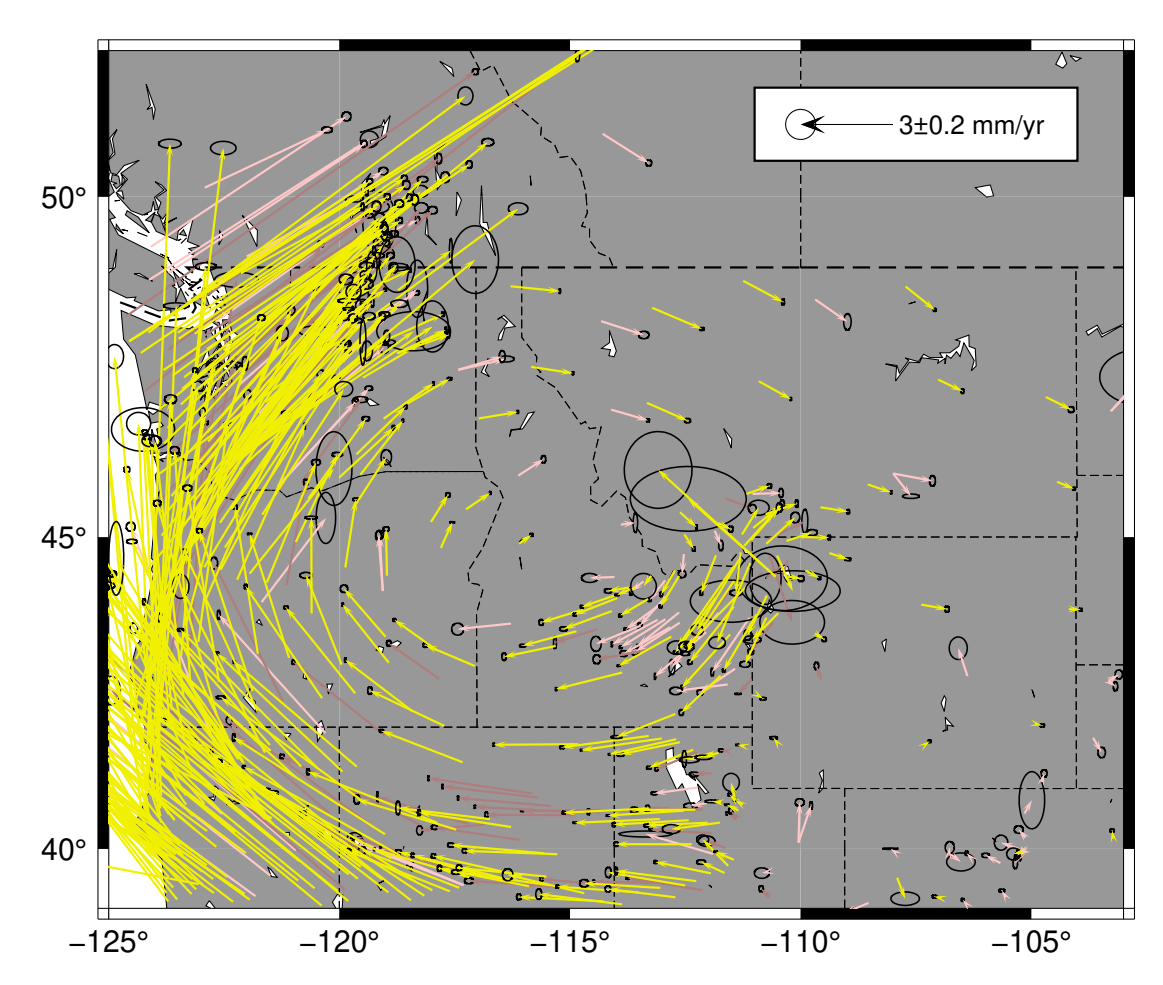


Figure 12: Same as Figure 8 except for Western Central United States. Only velocities with horizontal standard deviations less than 1 mm/yr are shown. Anomalous vectors at longitude 250° are in the Yellowstone National Park and most likely are showing volcanic processes.

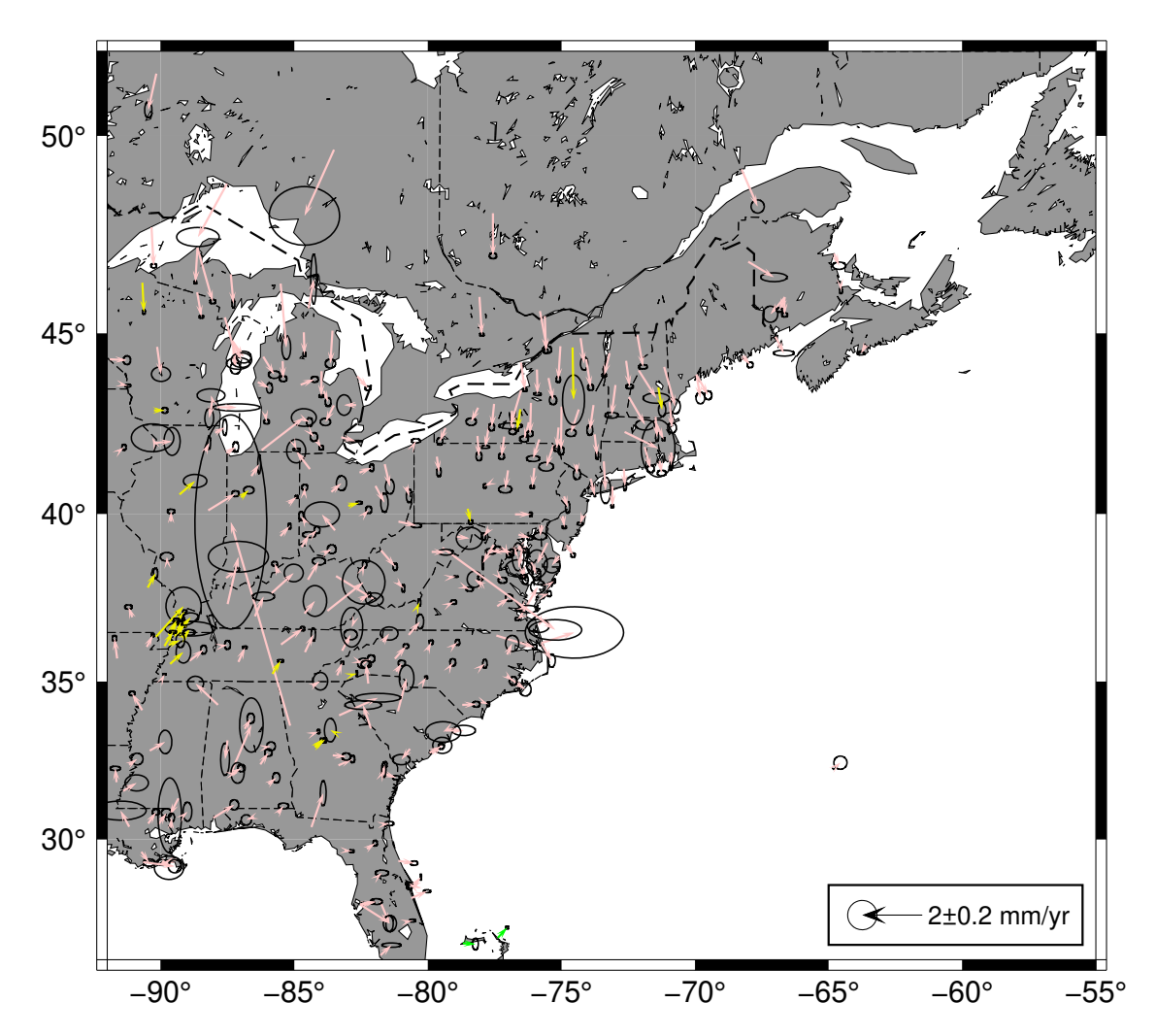


Figure 13: Same as Figure 8 except for the Eastern United States. Only velocities with horizontal standard deviations less than 2 mm/yr are shown. The systematic velocity of sites in the Northeast and central US show deviations for current GIA models in the horizontal velocities.

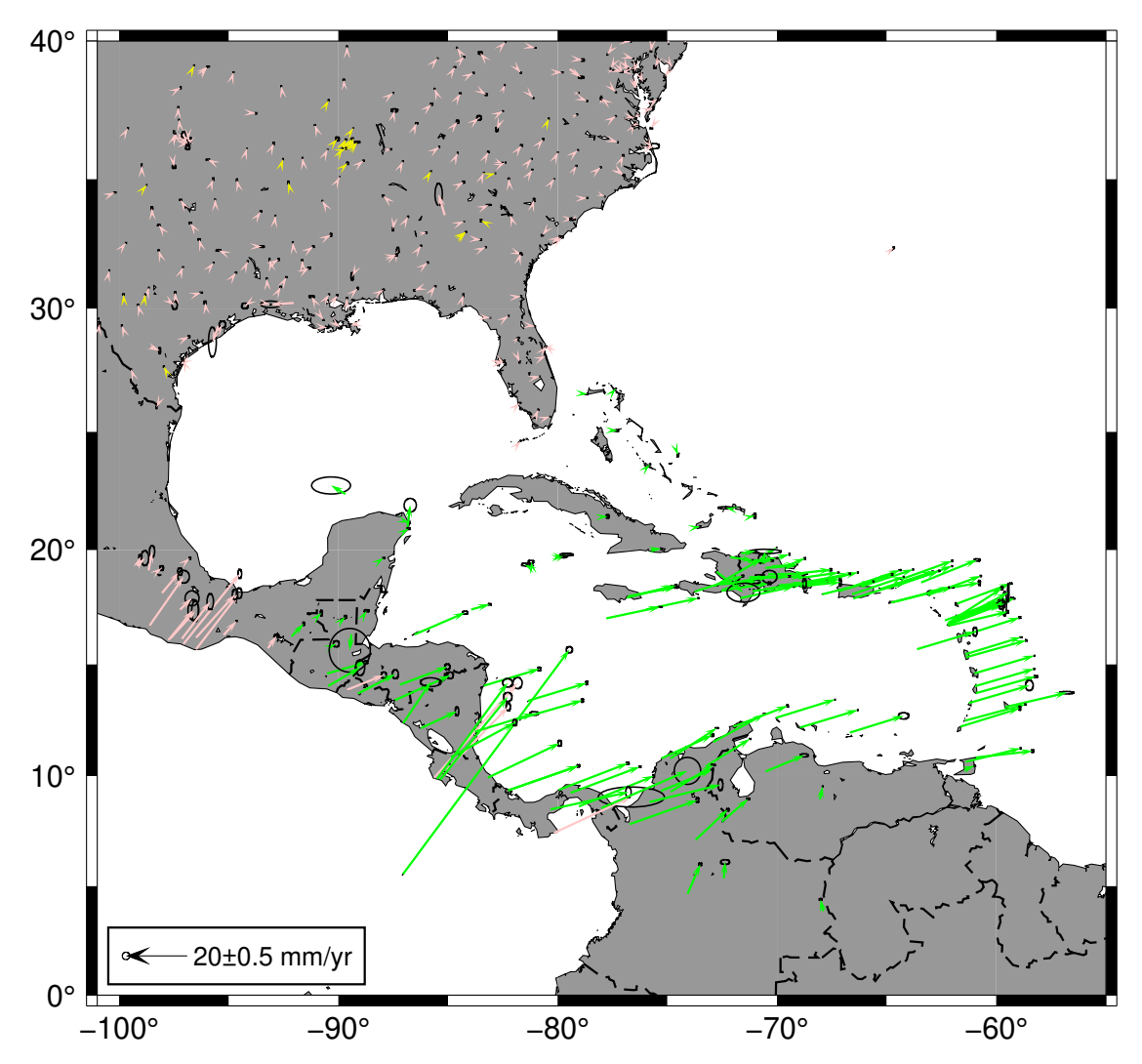


Figure 14: Same as Figure 8 except for the Caribbean region. Only velocities with horizontal standard deviations less than 5 mm/yr are shown.

Earthquake Analyses: 2025/03/15-2025/09/15

We use the NEIC catalog to search for earthquakes that could cause coseismic offsets at the sites analyzed by the GAGE analysis centers. Of the 20 earthquakes examined during this quarter, two generated coseismic offsets. The two earthquakes are EQ77 ANSS(ComCat) us7000qd1y mww7.3 Sand Point, Alaska; date and time 2025/07/16 20:38 (epicenter 54.5489°N, 160.4717°W) and EQ78 ANSS(ComCat) us6000qw60 mww8.8 Kamchatka Peninsula; Date and time 2025/07/29 23:25 (epicenter 52.5300°N, 160.1648°E). The largest offset from EQ77 was at AC12 -22.57 mm E, -44.43 mm N, with four sites showing displacements

greater than 10 mm. The largest offset from EQ78 was at AC60 -11.12 mm E, 0.16 mm N. It was the only site showing more than 10 mm displacement.

Antenna and other discontinuity events.

Antenna swaps at 37 sites have been added to the list of offsets estimated when fitting velocities and other parameters to the CWU time series. These offsets were spread throughout the quarter. An additional 4 breaks were added to the All NOTA unkn.eq file.

Anomalous sites

The following sites have been noted as having anomalous motions during this quarter. We updated the ACC_GAGE website to show times of earthquakes, antenna changes, and offsets for unknown reasons. Plots for CWU are now generated with and without offsets (computed from the Kalman filter time series analysis) removed. The landing page for http://geoweb.mit.edu/~tah/ACC GAGE/ now has the following explanation.

Analyses from Central Washington University (CWU). Series are:

NMT -- Old plots from New Mexico Tech Analyses (Ends 9/15/2018).

-- Old plots from Combined NMT+CWU analyses (Ends 9/15/2108). **PBO**

CWURAW -- Raw time series with linear trend removed

CWUOFF -- Time series with linear trend and offsets from cwu,kalts nam14.off removed

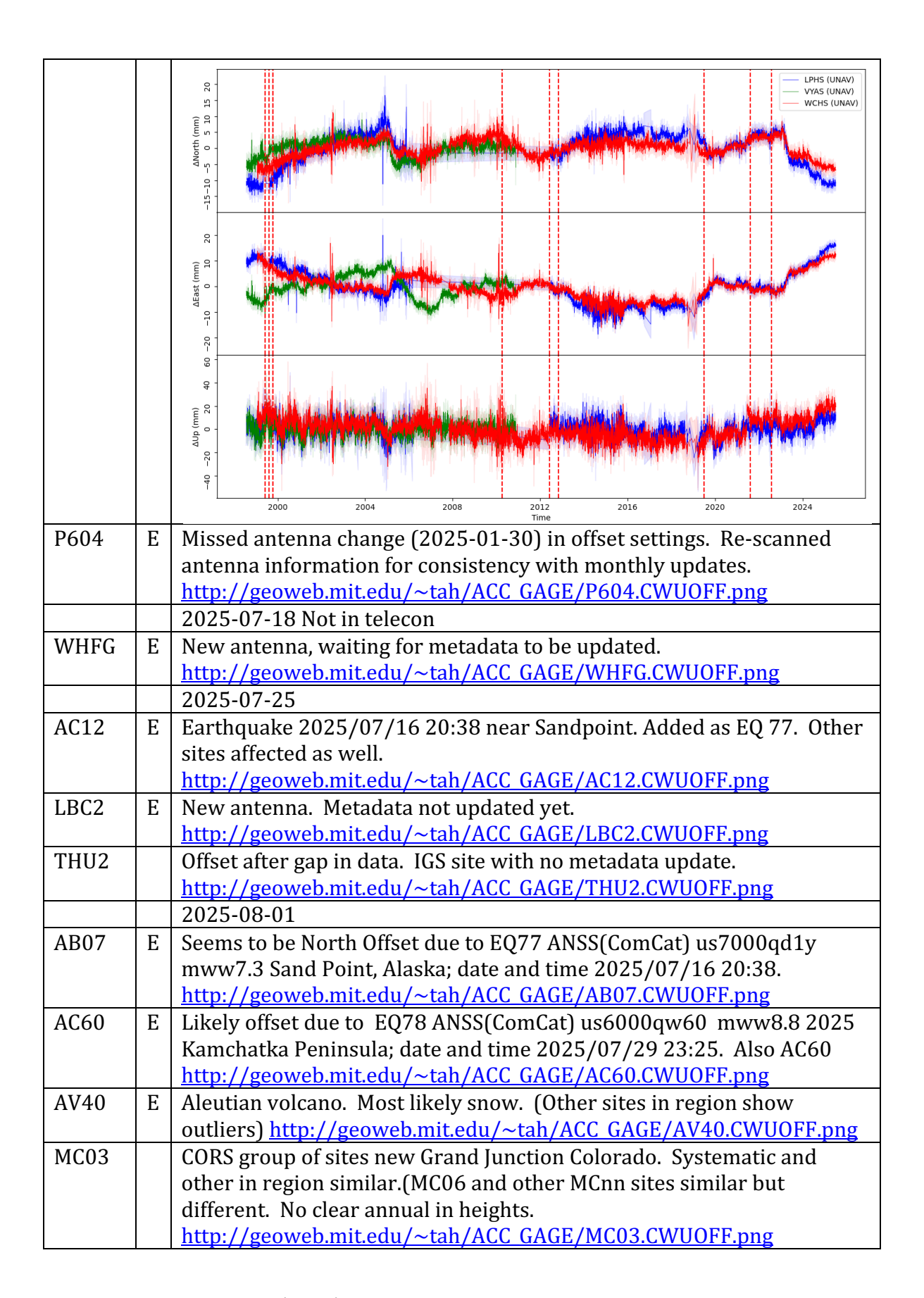
Vertical lines denote times of offsets in time series:

Purple, solid: Earthquakes (OffEq ! EQ) Blue, dotted: Antenna changes (Break! AN)

Cyan, dashed: Breaks for unknown reasons (Break! UN)

N after site name means NOTA operated site, U means UNAVCO/Earthscope log file.

| Site | N | Issues related to site |
|------|---|--|
| | | 2025-07-11 |
| CHOW | | Site in Central Valley, compare to P307 only 20km away. Effects of |
| | | ground water changes. Only log at SOPAC. |
| | | http://geoweb.mit.edu/~tah/ACC GAGE/CHOW.CWUOFF.png |
| | | http://geoweb.mit.edu/~tah/ACC_GAGE/P307.CWU0FF.png |
| LPHS | | Near LA, systematic. Share some behaviors with VYAS (gone) and |
| | | WCHS. No site photos but seems to be between two buildings. |
| | | http://geoweb.mit.edu/~tah/ACC GAGE/LPHS.CWUOFF.png |



| NIST | | GS site. Recently back online after antenna change. Seems to be earlier (2013 11 22) break in North. No meta data change at the time. | | | | | | | |
|------|---|--|--|--|--|--|--|--|--|
| | | http://geoweb.mit.edu/~tah/ACC_GAGE/NIST.CWUOFF.png | | | | | | | |
| P827 | N | ewer affiliate site in Centralia WA. Has a strong tidal-like signal in | | | | | | | |
| | | height. http://geoweb.mit.edu/~tah/ACC_GAGE/P827.CWUOFF.png | | | | | | | |
| RNCH | Е | Parkfield site with growing annual in East and now north. | | | | | | | |
| | | http://geoweb.mit.edu/~tah/ACC_GAGE/RNCH.CWUOFF.png | | | | | | | |
| | | 2025-08-08 | | | | | | | |
| AB18 | N | Interesting East behavior. Likely to be real. | | | | | | | |
| | | http://geoweb.mit.edu/~tah/ACC_GAGE/AB18.CWUOFF.png | | | | | | | |
| AB22 | N | "Continuous" North skewness. Looks like offset in North after gap but | | | | | | | |
| | | no metadata change. | | | | | | | |
| | | http://geoweb.mit.edu/~tah/ACC_GAGE/AB22.CWUOFF.png | | | | | | | |
| AC09 | N | Systematic but site ~100 km away don't show this behavior (EYAC, | | | | | | | |
| | | AB35, AC29). All show same annual except AC29 (on island) is lower | | | | | | | |
| | | seasonal amplitude until 2024 then is same as others. | | | | | | | |
| | | 8 — EYAC (UNAV) | | | | | | | |
| | | — AC09 (UNAV) — AB35 (UNAV) | | | | | | | |
| | | ayorth (mm) ACC50 (MMA) | | | | | | | |
| | | o o o o o o o o o o o o o o o o o o o | | | | | | | |
| | | -30 | | | | | | | |
| | | Q 1 | | | | | | | |
| | | 8- | | | | | | | |
| | | Que se la companya de la companya del companya de la companya del companya de la | | | | | | | |
| | | Ačest (mm) | | | | | | | |
| | | P. Committee and the committee of the co | | | | | | | |
| | | -79 | | | | | | | |
| | | 8 | | | | | | | |
| | | e 2 2 2 2 2 2 2 2 2 2 2 2 2 2 2 2 2 2 2 | | | | | | | |
| | | ο o o o o o o o o o o o o o o o o o o o | | | | | | | |
| | | 92 | | | | | | | |
| | | Q- | | | | | | | |
| | | 2016 2018 2020 2022 2024 Time | | | | | | | |
| 10:5 | | http://geoweb.mit.edu/~tah/ACC_GAGE/AC09.CWU0FF.png | | | | | | | |
| AC63 | N | Offset in 2018/01/24 appears due to EQ44 but not in current distance | | | | | | | |
| | | range. Offset looks "slow" with accumulation over a few days. In plot | | | | | | | |
| | | AB37 (South of AC63 and AC72) is in earthquake offset list (-4.89±0.42 | | | | | | | |
| | | -1.93±0.40 mm, dNE). AC71 may also be offset. Note also how | | | | | | | |
| | | correlated the height changes are. | | | | | | | |

| | | AB37 (UNAV) — AC63 (UNAV) — AC72 (UNAV) |
|------|----------|--|
| | | -15 -10 -5 0 9 5 10 4185 |
| | | -40 -20 0 20 40 |
| | | 2017-09 2017-11 2018-01 2018-03 2018-05 2018-07 2018-09 2018-11 2019-01 Time |
| | | http://geoweb.mit.edu/~tah/ACC_GAGE/AC63.CWUOFF.png 2025-08-15 |
| KYBO | | CORS site on building Byrlington KY. Strange change and east offset. |
| KIDO | | http://geoweb.mit.edu/~tah/ACC_GAGE/KYBO.CWUOFF.png |
| КҮМН | | CORS site. Failed antenna. |
| | | http://geoweb.mit.edu/~tah/ACC_GAGE/KYMH.CWUOFF.png |
| TPOG | Е | New antenna with old meta data. |
| | | http://geoweb.mit.edu/~tah/ACC_GAGE/TPOG.CWUOFF.png |
| | | 2025-08-22 (not in monthly) |
| ARHP | | Site in Texas, East offset (check to see if persists) |
| | | http://geoweb.mit.edu/~tah/ACC_GAGE/ARHP.CWUOFF.png |
| GV07 | | Galápagos Island recently back online after long gap. |
| | | http://geoweb.mit.edu/~tah/ACC_GAGE/GV07.CWU0FF.png |
| | | http://geoweb.mit.edu/~tah/ACC_GAGE/GV10.CWUOFF.png |
| MCOO | | 2025-08-29 Not in telecon |
| MC08 | | Jump in East. See if it continues. Has had outliers before. Just a few days off. |
| | | https://geoweb.mit.edu/~tah/ACC_GAGE/MC08.CWU0FF.png |
| MORP | | IGS Site In England East offset. Seems to returned to original position. |
| | | https://geoweb.mit.edu/~tah/ACC_GAGE/MORP.CWUOFF.png |
| SPRG | | PANGA site in Washingtom State, west of Spokane. Could be vegetation |
| | | or failing antenna. |
| | | https://geoweb.mit.edu/~tah/ACC_GAGE/SPRG.CWUOFF.png |
| TXTI | | CORS site in Texas – could be oil pumping? |
| | | https://geoweb.mit.edu/~tah/ACC_GAGE/TXTI.CWUOFF.png |
| WVBU | | CORS site in Virginia with antenna program but WVCV 60 km away has |
| | | clean time series but large velocity. Not clear why. |
| İ | <u> </u> | * Long Lat Evel Nvel E +- N +- Hvel H +- Site |

| <u> </u> | | |
|----------|----|---|
| | | * deg deg mm/yr mm/yr mm/yr mm/yr mm/yr mm/yr |
| | | 281.08650 39.33801 0.48 -0.01 0.10 0.10 -2.31 0.27 WVBU 280.54305 39.01531 3.78 -2.75 0.36 0.14 -2.68 0.14 WVCV |
| | | 277.57529 38.42296 0.05 0.12 0.03 0.05 -2.34 0.15 WVHU |
| | | 280.14159 38.89570 0.49 -0.01 0.05 0.03 -1.76 0.10 WVNR |
| | | 278.86783 37.99826 0.20 -0.19 0.02 0.05 -2.54 0.35 WVOH |
| | | 278.24865 38.94136 0.47 -0.55 0.03 0.05 -2.13 0.11 WVRA |
| | | https://geoweb.mit.edu/~tah/ACC_GAGE/WVBU.CWUOFF.png |
| | | 2025-09-05 |
| UPTC | | Maybe be failing. Site in NorthEast. |
| | | https://geoweb.mit.edu/~tah/ACC_GAGE/UPTC.CWUOFF.png |
| MTCC | - | 2025-09-12 |
| MTGG | E | California site, strange systematics, out of phase with LKHG 11 km |
| | | away, P482 5 km away does no show pattern. No photos of MTGG but |
| | | LKHG has one photo and looks like seismic station. Both listed as |
| | | shallow foundation mast. |
| | | https://geoweb.mit.edu/~tah/ACC_GAGE/MTGG.CWUOFF.png |
| | | https://geoweb.mit.edu/~tah/ACC GAGE/LKHG.CWUOFF.png |
| NYLV | | CORS site in NY on building. Looks like it is disturbed. Check again |
| | | later. Came back after about week? |
| | | https://geoweb.mit.edu/~tah/ACC_GAGE/NYLV.CWUOFF.png |
| P029 | | Site near Colorado Springs. Systematic. |
| | | https://geoweb.mit.edu/~tah/ACC_GAGE/P029.CWU0FF.png |
| ZLC1 | | CORS WAAS site in Salt Lake City, very systematic can correlated with |
| ZECI | | SLCU a 1.5 km away but not with other sires 12 km (RBUT) away. |
| | | https://geoweb.mit.edu/~tah/ACC GAGE/ZLC1.CWUOFF.png |
| | | 2025-09-19 Not in Monthly |
| KYVW | Е | Earthscope log, Looks like receiver has failed. Site in Southern CA. |
| IXIVV | | https://geoweb.mit.edu/~tah/ACC GAGE/KYVW.CWUOFF.png |
| VIKH | | CORS site in US Virgin Islands. 28 mm height 2024/09/17. No obvious |
| VIIXII | | reason. https://geoweb.mit.edu/~tah/ACC GAGE/VIKH.CWUOFF.png |
| | | 2025-09-26 Not in telecon |
| P039 | N | Offsets in North and East. Site near Clayton, CO. No new metadata since |
| 1037 | 11 | 2019? https://geoweb.mit.edu/~tah/ACC GAGE/P039.CWU0FF.png |
| | | 2025-10-03 |
| P435 | N | 10 mm outlier in East. Has done this once before; check again in a few |
| P433 | IN | |
| | | days. Was single outlier; skewness in north so probably weather. |
| | - | https://geoweb.mit.edu/~tah/ACC_GAGE/P435.CWUOFF.png |
| YWG1 | | Canadian site near Lake Winnipeg: East oscillations. CORS WAAS |
| | | station. https://geoweb.mit.edu/~tah/ACC_GAGE/YWG1.CWU0FF.png |
| | 1 | 2025-10-10 |
| PUPU | E | Site in Washington State South of Vancouver Island. ~20 mm NE offset |
| | | when site comes back online. No new meta data. Also earlier offset in |
| | | 2013. See what happens. Added UNKN breaks. |
| | 1 | https://geoweb.mit.edu/~tah/ACC GAGE/PUPU.CWUOFF.png |
| | | 2025-10-17 not in Montly/telecon |
| AC81 | Е | New site and first point is offset. Point removed from time series. |
| | | 1 |

| | https://geoweb.mit.edu/~tah/ACC_GAGE/AC81.CWUOFF.png |
|------|--|
| RG24 | RioGrand site, skewed (another example). |
| | https://geoweb.mit.edu/~tah/ACC_GAGE/RG24.CWUOFF.png |
| | |

GNSS Rapid processing

Since 2021/10/20, CWU has generated a combined GPS and Galileo rapid solution because JPL has made available orbit and clock files from a global GPS and Galileo solution. These solutions are experimental, and for a number of sites, there are systematic mean differences in position between the GPS-only and the combined solutions. For this reason, these combined solutions are not distributed through the EarthScope GAGE products portal. Initially, there were inconsistencies in the GPS-only and combined analyses (e.g., elevation angle cutoff) that affected the comparison of the results, specifically when comparing mean positions and WRMS scatters of the fits to linear trends. Starting on 2024/03/26, these inconsistencies were resolved and since that time, a direct comparison of the GPS-only and combined GPS and Galileo solutions is possible. Results of the comparisons are reported daily to the GAGE ACS email list. With nine months of consistently processed results available, we compare the results below. The current analysis used 973 stations with up to 569 days of comparison. The median NEU scatters for the GPS+GAL solutions are 0.88, 0.93, and 5.00 mm. The corresponding values from the common GPS-only solutions are 0.95, 0.98, and 5.32 mm, slightly larger than those from the GPS+GAL solution.

Table 4: Mean differences between GPS-only and GPS+Galileo rapid solutions. Differences are taken as GPS+GAL minus GPS-only position estimates. The largest 10 positive and negative differences in Up, North, and East are shown. The sig column is the standard deviation of the mean (assuming white noise statistics), wrms is the weighted root-mean-square scatter about the mean, and nrms is the normalized root mean square $(\sqrt{\chi^2/f})$.

| CWU G | NSSR | Anal | lysis Thu O | ct 16 22 | :26:58 | EDT 20 |) 25 | | | |
|-------|------|------|-------------|----------|--------|--------|----------------|-------|----------------|--------|
| Stat | enu | # | MeanDiff | sig | wrms | nrms | Receiver | | Antenna | Radome |
| | | | (mm) | (mm) | (mm) | | | | | |
| FLIN | U | 546 | -13.18 | 0.10 | 2.27 | 0.2 | SEPT POLARX5 | | N0V750.R4 | NOVS |
| SASK | U | 548 | -12.17 | 0.09 | 2.11 | 0.2 | JAVAD TRE_G3TH | DELTA | N0V750.R4 | NOVS |
| ARBT | U | 356 | -8.90 | 0.24 | 4.60 | 0.5 | TRIMBLE NETR9 | | TRM115000.00 | NONE |
| HDIL | U | 102 | -7.50 | 0.62 | 6.28 | 0.5 | SEPT POLARX5 | | TRM59800.80 | SCIT |
| PTRF | U | 346 | -7.09 | 0.24 | 4.48 | | SEPT POLARX5S | | SEPCH0KE_B3E6 | SPKE |
| SELD | U | 468 | -6.41 | 0.23 | 4.96 | 0.5 | SEPT POLARX5 | | TRM159800.00 | SCIT |
| 1LSU | U | 302 | -6.30 | 0.36 | 6.29 | 0.5 | TRIMBLE ALLOY | | TRM115000.00 | NONE |
| CN29 | U | 374 | -6.21 | 0.48 | 9.36 | 0.6 | TRIMBLE NETR9 | | TRM59800.99 | SCIT |
| Y0RK | U | 323 | -5.91 | 1.55 | 27.77 | 1.0 | TRIMBLE ALLOY | | TRM115000.10 | NONE |
| MHMS | U | 545 | -5.66 | 0.14 | 3.17 | 0.3 | SEPT POLARX5 | | TWIVC6050 | SCIT |
| | | | | | | | | | | |
| ARML | U | 397 | 5.88 | 0.18 | 3.68 | 0.4 | SEPT POLARX5 | | SEPPOLANT_X_MF | NONE |
| LCHS | U | 402 | 5.97 | 0.21 | 4.12 | 0.4 | SEPT POLARX5 | | SEPPOLANT_X_MF | NONE |
| P669 | U | 548 | 6.10 | 0.18 | 4.11 | 0.3 | SEPT POLARX5 | | TWIVC6050 | SCIS |
| CHZZ | U | 546 | 6.23 | 0.31 | 7.20 | 0.5 | TRIMBLE NETR9 | | TRM59800.80 | SCIT |
| LMCN | U | 346 | 6.50 | 0.23 | 4.37 | 0.5 | TRIMBLE ALLOY | | TRM115000.00 | NONE |
| NWCC | U | 37 | 6.56 | 0.40 | 2.45 | 0.3 | SEPT POLARX5 | | SEPPOLANT_X_MF | NONE |
| HCES | U | 98 | 6.67 | 0.36 | 3.54 | | SEPT POLARX5 | | SEPPOLANT_X_MF | NONE |
| MCTY | U | 399 | 7.89 | 0.24 | 4.81 | 0.5 | SEPT POLARX5 | | SEPPOLANT_X_MF | NONE |
| | | | | | | | | | | |

| P312 COLA | U U | 544 544 | 10.14 14.33 | 1.64 0.49 | 38.24 11.49 | | TRIMBLE NETR9 TRIMBLE ALLOY | TRM59800.80 TRM55971.00 | SCIT NONE |
|---|---------------------------------|---|--|--|--|--|---|--|--|
| Stat | enu | # | MeanDiff (mm) | sig (mm) | wrms (mm) | nrms | Receiver | Antenna | Radome |
| LONG | N | 541 | -2.40 | 0.13 | 3.13 | 1.1 | SEPT POLARX5 | TWIVC6050 | SCPL |
| COLA | N | 544 | -1.89 | 0.07 | 1.73 | 0.8 | TRIMBLE ALLOY | TRM55971.00 | NONE |
| P669 | N | 548 | -1.58 | 0.03 | 0.82 | 0.3 | SEPT POLARX5 | TWIVC6050 | SCIS |
| SELD | N | 468 | -1.51 | 0.05 | 1.01 | 0.3 | SEPT POLARX5 | TRM159800.00 | SCIT |
| P224 | N | 547 | -1.47 | 0.04 | 0.87 | 0.3 | TRIMBLE NETR9 | TRM59800.00 | SCIT |
| MHMS | N | 545 | -1.40 | 0.03 | 0.76 | 0.3 | SEPT POLARX5 | TWIVC6050 | SCIT |
| P388 | N | 548 | -1.35 | 0.02 | 0.42 | 0.1 | SEPT POLARX5 | TRM59800.00 | SCIT |
| AB48 | N | 6 | -1.32 | 1.25 | 1.14 | 0.3 | SEPT POLARX5 | TRM29659.00 | SCIT |
| AC34 | N | 325 | -1.24 | 0.04 | 0.80 | 0.3 | SEPT POLARX5 | TRM29659.00 | SCIT |
| P312 | N | 544 | -1.21 | 0.26 | 6.17 | | TRIMBLE NETR9 | TRM59800.80 | SCIT |
| P794 | N | 464 | 1.17 | 0.02 | 0.51 | | SEPT POLARX5 | TRM59800.00 | SCIT |
| P399 | N | 444 | 1.18 | 0.02 | 0.46 | | SEPT POLARX5 | TRM59800.99 | SCIT |
| KYMH | N | 333 | 1.23 | 0.06 | 1.10 | | TRIMBLE ALLOY | TRM115000.00 | NONE |
| GOLD | N | 541 | 1.24 | 0.02 | 0.41 | | JAVAD TRE_G3TH DELTA | · - | NONE |
| P156 | N | 425 | 1.36 | 0.11 | 2.35 | | SEPT POLARX5 | TRM59800.80 | SCIT |
| 0SPA | N | 355 | 1.46 | 0.07 | 1.25 | | SEPT POLARX5 | TWIVC6150 | SCIS |
| P215 | N | 471 | 1.61 | 0.04 | 0.98 | | SEPT POLARX5 | TRM59800.80 | SCIT |
| P385 | N | 533 | 1.92 | 0.10 | 2.41 | | SEPT POLARX5 | TRM59800.80 | SCIT |
| P252 | N | 53 | 2.28 | 0.20 | 1.49 | | TRIMBLE NETR9 | TRM29659.00 | SCIT |
| NNVN | N | 410 | 2.85 | 0.25 | 5.03 | 1.8 | ALERTGEO RESOLUTE | LEIAR20 | LEIM |
| Stat | enu | # | MeanDiff (mm) | sig (mm) | wrms (mm) | nrms | Receiver | Antenna | Radome |
| CAT3 | Е | 548 | -2 . 57 | 0.29 | 6.79 | αΩ | TRIMBLE ALLOY | TRM59800.80 | SCIT |
| | | | -2.37 | 0.29 | 0.79 | 0.0 | | | SCIS |
| | | | 1 01 | $\alpha \alpha I$ | A 00 | aο | CEDT DALABVE | | |
| P669 | E | 548 | -1.81 1.44 | 0.04 | 0.88 | | SEPT POLARX5 | TWIVC6050 | |
| KVTX | Ε | 549 | -1.44 | 0.03 | 0.65 | 0.3 | SEPT POLARX5 | TRM59800.99 | SCIT |
| KVTX RDF2 | E E | 549 74 | -1.44 -1.42 | 0.03 0.18 | 0.65 1.51 | 0.3 0.5 | SEPT POLARX5 TRIMBLE NETR9 | TRM59800.99 TRM57971.00 | SCIT NONE |
| KVTX RDF2 AB48 | E E E | 549 74 6 | -1.44 -1.42 -1.35 | 0.03 0.18 0.79 | 0.65 1.51 0.63 | 0.3 0.5 0.3 | SEPT POLARX5 TRIMBLE NETR9 SEPT POLARX5 | TRM59800.99 TRM57971.00 TRM29659.00 | SCIT NONE SCIT |
| KVTX RDF2 AB48 TFN0 | E E E | 549 74 6 357 | -1.44 -1.42 -1.35 -1.34 | 0.03 0.18 0.79 0.09 | 0.65 1.51 0.63 1.70 | 0.3 0.5 0.3 0.7 | SEPT POLARX5 TRIMBLE NETR9 SEPT POLARX5 SEPT POLARX5 | TRM59800.99 TRM57971.00 TRM29659.00 SEPCHOKE_B3E6 | SCIT NONE SCIT SPKE |
| KVTX RDF2 AB48 TFN0 P011 | E E E E | 549 74 6 357 547 | -1.44 -1.42 -1.35 -1.34 -1.32 | 0.03 0.18 0.79 0.09 0.03 | 0.65 1.51 0.63 1.70 0.70 | 0.3 0.5 0.3 0.7 0.4 | SEPT POLARX5 TRIMBLE NETR9 SEPT POLARX5 SEPT POLARX5 SEPT POLARX5 | TRM59800.99 TRM57971.00 TRM29659.00 SEPCHOKE_B3E6 TRM59800.80 | SCIT NONE SCIT SPKE SCIT |
| KVTX RDF2 AB48 TFN0 P011 P187 | E E E E | 549 74 6 357 547 547 | -1.44 -1.42 -1.35 -1.34 -1.32 | 0.03 0.18 0.79 0.09 0.03 0.12 | 0.65 1.51 0.63 1.70 0.70 2.78 | 0.3 0.5 0.3 0.7 0.4 0.9 | SEPT POLARX5 TRIMBLE NETR9 SEPT POLARX5 SEPT POLARX5 SEPT POLARX5 SEPT POLARX5 | TRM59800.99 TRM57971.00 TRM29659.00 SEPCHOKE_B3E6 TRM59800.80 TRM59800.99 | SCIT NONE SCIT SPKE SCIT SCIT |
| KVTX RDF2 AB48 TFN0 P011 P187 P051 | E E E E E | 549 74 6 357 547 547 544 | -1.44 -1.42 -1.35 -1.34 -1.32 -1.22 -1.21 | 0.03 0.18 0.79 0.09 0.03 0.12 0.02 | 0.65 1.51 0.63 1.70 0.70 2.78 0.41 | 0.3 0.5 0.3 0.7 0.4 0.9 | SEPT POLARX5 TRIMBLE NETR9 SEPT POLARX5 SEPT POLARX5 SEPT POLARX5 SEPT POLARX5 SEPT POLARX5 | TRM59800.99 TRM57971.00 TRM29659.00 SEPCHOKE_B3E6 TRM59800.80 TRM59800.99 TRM59800.00 | SCIT NONE SCIT SPKE SCIT SCIT SCIT |
| KVTX RDF2 AB48 TFN0 P011 P187 | E E E E | 549 74 6 357 547 547 | -1.44 -1.42 -1.35 -1.34 -1.32 | 0.03 0.18 0.79 0.09 0.03 0.12 | 0.65 1.51 0.63 1.70 0.70 2.78 | 0.3 0.5 0.3 0.7 0.4 0.9 | SEPT POLARX5 TRIMBLE NETR9 SEPT POLARX5 SEPT POLARX5 SEPT POLARX5 SEPT POLARX5 | TRM59800.99 TRM57971.00 TRM29659.00 SEPCHOKE_B3E6 TRM59800.80 TRM59800.99 | SCIT NONE SCIT SPKE SCIT SCIT |
| KVTX RDF2 AB48 TFN0 P011 P187 P051 TNAL P505 | E E E E E | 549 74 6 357 547 547 544 227 | -1.44 -1.42 -1.35 -1.34 -1.32 -1.22 -1.21 -1.15 | 0.03 0.18 0.79 0.09 0.03 0.12 0.02 0.07 | 0.65 1.51 0.63 1.70 0.70 2.78 0.41 1.03 | 0.3 0.5 0.3 0.7 0.4 0.9 0.2 0.4 | SEPT POLARX5 TRIMBLE NETR9 SEPT POLARX5 SEPT POLARX5 SEPT POLARX5 SEPT POLARX5 SEPT POLARX5 TRIMBLE NETR9 TRIMBLE NETR9 | TRM59800.99 TRM57971.00 TRM29659.00 SEPCHOKE_B3E6 TRM59800.80 TRM59800.99 TRM59800.00 | SCIT NONE SCIT SPKE SCIT SCIT SCIT NONE |
| KVTX RDF2 AB48 TFN0 P011 P187 P051 TNAL | E E E E E E E | 549 74 6 357 547 547 544 227 | -1.44 -1.42 -1.35 -1.34 -1.32 -1.22 -1.21 -1.15 | 0.03 0.18 0.79 0.09 0.03 0.12 0.02 0.07 | 0.65 1.51 0.63 1.70 0.70 2.78 0.41 1.03 | 0.3 0.5 0.3 0.7 0.4 0.9 0.2 0.4 | SEPT POLARX5 TRIMBLE NETR9 SEPT POLARX5 SEPT POLARX5 SEPT POLARX5 SEPT POLARX5 SEPT POLARX5 TRIMBLE NETR9 | TRM59800.99 TRM57971.00 TRM29659.00 SEPCHOKE_B3E6 TRM59800.80 TRM59800.99 TRM59800.00 TRM57971.00 | SCIT NONE SCIT SPKE SCIT SCIT SCIT NONE |
| KVTX RDF2 AB48 TFN0 P011 P187 P051 TNAL P505 | E E E E E E E | 549 74 6 357 547 547 544 227 | -1.44 -1.42 -1.35 -1.34 -1.32 -1.22 -1.21 -1.15 | 0.03 0.18 0.79 0.09 0.03 0.12 0.02 0.07 | 0.65 1.51 0.63 1.70 0.70 2.78 0.41 1.03 | 0.3 0.5 0.3 0.7 0.4 0.9 0.2 0.4 | SEPT POLARX5 TRIMBLE NETR9 SEPT POLARX5 SEPT POLARX5 SEPT POLARX5 SEPT POLARX5 SEPT POLARX5 TRIMBLE NETR9 TRIMBLE NETR9 SEPT POLARX5 TRIMBLE ALLOY | TRM59800.99 TRM57971.00 TRM29659.00 SEPCHOKE_B3E6 TRM59800.80 TRM59800.00 TRM57971.00 TRM59800.80 | SCIT NONE SCIT SPKE SCIT SCIT SCIT NONE |
| KVTX RDF2 AB48 TFN0 P011 P187 P051 TNAL P505 KIR0 | E E E E E | 549 74 6 357 547 547 544 227 457 539 | -1.44 -1.42 -1.35 -1.34 -1.32 -1.22 -1.21 -1.15 | 0.03 0.18 0.79 0.09 0.03 0.12 0.02 0.07 | 0.65 1.51 0.63 1.70 0.70 2.78 0.41 1.03 | 0.3 0.5 0.3 0.7 0.4 0.9 0.2 0.4 | SEPT POLARX5 TRIMBLE NETR9 SEPT POLARX5 SEPT POLARX5 SEPT POLARX5 SEPT POLARX5 SEPT POLARX5 TRIMBLE NETR9 TRIMBLE NETR9 SEPT POLARX5 | TRM59800.99 TRM57971.00 TRM29659.00 SEPCHOKE_B3E6 TRM59800.80 TRM59800.99 TRM59800.00 TRM57971.00 TRM57971.00 | SCIT NONE SCIT SPKE SCIT SCIT SCIT NONE SCIT OSOD |
| KVTX RDF2 AB48 TFN0 P011 P187 P051 TNAL P505 KIR0 PAMS P740 KOKB | | 549 74 6 357 547 547 544 227 457 539 344 536 407 | -1.44 -1.42 -1.35 -1.34 -1.32 -1.22 -1.21 -1.15 1.03 1.04 1.06 1.08 1.14 | 0.03 0.18 0.79 0.09 0.03 0.12 0.02 0.07 | 0.65 1.51 0.63 1.70 0.70 2.78 0.41 1.03 2.70 0.68 0.70 1.33 0.99 | 0.3 0.5 0.3 0.7 0.4 0.9 0.2 0.4 1.4 0.3 0.5 | SEPT POLARX5 TRIMBLE NETR9 SEPT POLARX5 SEPT POLARX5 SEPT POLARX5 SEPT POLARX5 SEPT POLARX5 TRIMBLE NETR9 TRIMBLE NETR9 SEPT POLARX5 TRIMBLE ALLOY SEPT POLARX5 SEPT POLARX5 | TRM59800.99 TRM57971.00 TRM29659.00 SEPCHOKE_B3E6 TRM59800.80 TRM59800.00 TRM57971.00 TRM59800.80 JAVRINGANT_DM TRM115000.00 | SCIT NONE SCIT SPKE SCIT SCIT SCIT NONE SCIT OSOD NONE SCIT NONE |
| KVTX RDF2 AB48 TFN0 P011 P187 P051 TNAL P505 KIR0 PAMS P740 KOKB ONSA | | 549 74 6 357 547 547 544 227 457 539 344 536 407 542 | -1.44 -1.42 -1.35 -1.34 -1.32 -1.22 -1.21 -1.15 1.03 1.04 1.06 1.08 1.14 1.24 | 0.03 0.18 0.79 0.09 0.03 0.12 0.02 0.07 0.13 0.03 0.04 0.06 0.05 0.03 | 0.65 1.51 0.63 1.70 0.70 2.78 0.41 1.03 2.70 0.68 0.70 1.33 0.99 0.72 | 0.3 0.5 0.3 0.7 0.4 0.9 0.2 0.4 1.4 0.3 0.5 0.5 | SEPT POLARX5 TRIMBLE NETR9 SEPT POLARX5 SEPT POLARX5 SEPT POLARX5 SEPT POLARX5 SEPT POLARX5 TRIMBLE NETR9 TRIMBLE NETR9 SEPT POLARX5 TRIMBLE ALLOY SEPT POLARX5 SEPT POLARX5 SEPT POLARX5 SEPT POLARX5 | TRM59800.99 TRM57971.00 TRM29659.00 SEPCHOKE_B3E6 TRM59800.80 TRM59800.00 TRM57971.00 TRM59800.80 JAVRINGANT_DM TRM115000.00 TRM59800.99 ASH701945G_M AOAD/M_B | SCIT NONE SCIT SPKE SCIT SCIT SCIT NONE SCIT OSOD NONE SCIT NONE OSOD |
| KVTX RDF2 AB48 TFN0 P011 P187 P051 TNAL P505 KIR0 KOKB ONSA P071 | | 549 74 6 357 547 547 544 227 457 539 344 536 407 | -1.44 -1.42 -1.35 -1.34 -1.32 -1.22 -1.21 -1.15 1.03 1.04 1.06 1.08 1.14 1.24 1.28 | 0.03 0.18 0.79 0.09 0.03 0.12 0.02 0.07 0.13 0.03 0.04 0.06 0.05 0.03 | 0.65 1.51 0.63 1.70 0.70 2.78 0.41 1.03 2.70 0.68 0.70 1.33 0.99 0.72 0.34 | 0.3 0.5 0.3 0.7 0.4 0.9 0.2 0.4 1.4 0.3 0.5 0.5 0.4 | SEPT POLARX5 TRIMBLE NETR9 SEPT POLARX5 SEPT POLARX5 SEPT POLARX5 SEPT POLARX5 SEPT POLARX5 TRIMBLE NETR9 TRIMBLE NETR9 SEPT POLARX5 TRIMBLE ALLOY SEPT POLARX5 SEPT POLARX5 SEPT POLARX5TR SEPT POLARX5TR SEPT POLARX5 | TRM59800.99 TRM57971.00 TRM29659.00 SEPCHOKE_B3E6 TRM59800.80 TRM59800.00 TRM57971.00 TRM59800.80 JAVRINGANT_DM TRM115000.00 TRM59800.99 ASH701945G_M | SCIT NONE SCIT SPKE SCIT SCIT SCIT NONE SCIT OSOD NONE SCIT NONE OSOD SCIT |
| KVTX RDF2 AB48 TFN0 P011 P187 P051 TNAL P505 KIR0 PAMS P740 KOKB ONSA P071 NDAP | | 549 74 6 357 547 547 544 227 457 539 344 536 407 542 545 548 | -1.44 -1.42 -1.35 -1.34 -1.32 -1.22 -1.21 -1.15 1.03 1.04 1.06 1.08 1.14 1.24 1.28 1.87 | 0.03 0.18 0.79 0.09 0.03 0.12 0.02 0.07 0.13 0.03 0.04 0.06 0.05 0.03 0.01 | 0.65 1.51 0.63 1.70 0.70 2.78 0.41 1.03 2.70 0.68 0.70 1.33 0.99 0.72 0.34 2.75 | 0.3 0.5 0.3 0.7 0.4 0.9 0.2 0.4 1.4 0.3 0.5 0.5 0.4 | SEPT POLARX5 TRIMBLE NETR9 SEPT POLARX5 SEPT POLARX5 SEPT POLARX5 SEPT POLARX5 SEPT POLARX5 TRIMBLE NETR9 TRIMBLE NETR9 SEPT POLARX5 TRIMBLE ALLOY SEPT POLARX5 SEPT POLARX5 SEPT POLARX5TR SEPT POLARX5TR SEPT POLARX5 TRIMBLE NETR9 | TRM59800.99 TRM57971.00 TRM29659.00 SEPCHOKE_B3E6 TRM59800.80 TRM59800.00 TRM57971.00 TRM59800.80 JAVRINGANT_DM TRM115000.00 TRM59800.99 ASH701945G_M AOAD/M_B | SCIT NONE SCIT SPKE SCIT SCIT SCIT NONE SCIT OSOD NONE SCIT NONE OSOD SCIT SCIT |
| KVTX RDF2 AB48 TFN0 P011 P187 P051 TNAL P505 KIR0 PAMS PAMS P0740 KOKB ONSA P071 NDAP EGAN | | 549 74 6 357 547 547 544 227 457 539 344 536 407 542 545 548 | -1.44 -1.42 -1.35 -1.34 -1.32 -1.22 -1.21 -1.15 1.03 1.04 1.06 1.08 1.14 1.24 1.28 1.87 1.97 | 0.03 0.18 0.79 0.09 0.03 0.12 0.02 0.07 0.13 0.03 0.04 0.05 0.03 0.01 0.12 0.13 | 0.65 1.51 0.63 1.70 0.70 2.78 0.41 1.03 2.70 0.68 0.70 1.33 0.99 0.72 0.34 2.75 3.07 | 0.3 0.5 0.3 0.7 0.4 0.9 0.2 0.4 1.4 0.3 0.5 0.5 0.4 0.2 | SEPT POLARX5 TRIMBLE NETR9 SEPT POLARX5 SEPT POLARX5 SEPT POLARX5 SEPT POLARX5 SEPT POLARX5 TRIMBLE NETR9 TRIMBLE NETR9 SEPT POLARX5 TRIMBLE ALLOY SEPT POLARX5 SEPT POLARX5TR SEPT POLARX5TR SEPT POLARX5TR SEPT POLARX5TR SEPT POLARX5 TRIMBLE NETR9 TRIMBLE NETR9 | TRM59800.99 TRM57971.00 TRM29659.00 SEPCHOKE_B3E6 TRM59800.80 TRM59800.00 TRM57971.00 TRM59800.80 JAVRINGANT_DM TRM15000.00 TRM59800.99 ASH701945G_M AOAD/M_B TRM59800.99 TRM59800.80 TRM59800.80 TRM59800.80 | SCIT NONE SCIT SPKE SCIT SCIT SCIT NONE SCIT NONE SCIT NONE SCIT NONE SCIT SCIT SCIT SCIT |
| KVTX RDF2 AB48 TFN0 P011 P187 P051 TNAL P505 KIR0 PAMS P740 KOKB ONSA P071 NDAP | | 549 74 6 357 547 547 544 227 457 539 344 536 407 542 545 548 | -1.44 -1.42 -1.35 -1.34 -1.32 -1.22 -1.21 -1.15 1.03 1.04 1.06 1.08 1.14 1.24 1.28 1.87 | 0.03 0.18 0.79 0.09 0.03 0.12 0.02 0.07 0.13 0.03 0.04 0.06 0.05 0.03 0.01 | 0.65 1.51 0.63 1.70 0.70 2.78 0.41 1.03 2.70 0.68 0.70 1.33 0.99 0.72 0.34 2.75 | 0.3 0.5 0.3 0.7 0.4 0.9 0.2 0.4 1.4 0.3 0.5 0.5 0.4 0.2 | SEPT POLARX5 TRIMBLE NETR9 SEPT POLARX5 SEPT POLARX5 SEPT POLARX5 SEPT POLARX5 SEPT POLARX5 TRIMBLE NETR9 TRIMBLE NETR9 SEPT POLARX5 TRIMBLE ALLOY SEPT POLARX5 SEPT POLARX5 SEPT POLARX5TR SEPT POLARX5TR SEPT POLARX5 TRIMBLE NETR9 | TRM59800.99 TRM57971.00 TRM29659.00 SEPCHOKE_B3E6 TRM59800.80 TRM59800.00 TRM57971.00 TRM59800.80 JAVRINGANT_DM TRM115000.00 TRM59800.99 ASH701945G_M AOAD/M_B TRM59800.99 TRM59800.99 TRM59800.90 | SCIT NONE SCIT SPKE SCIT SCIT SCIT NONE SCIT OSOD NONE SCIT NONE OSOD SCIT SCIT |

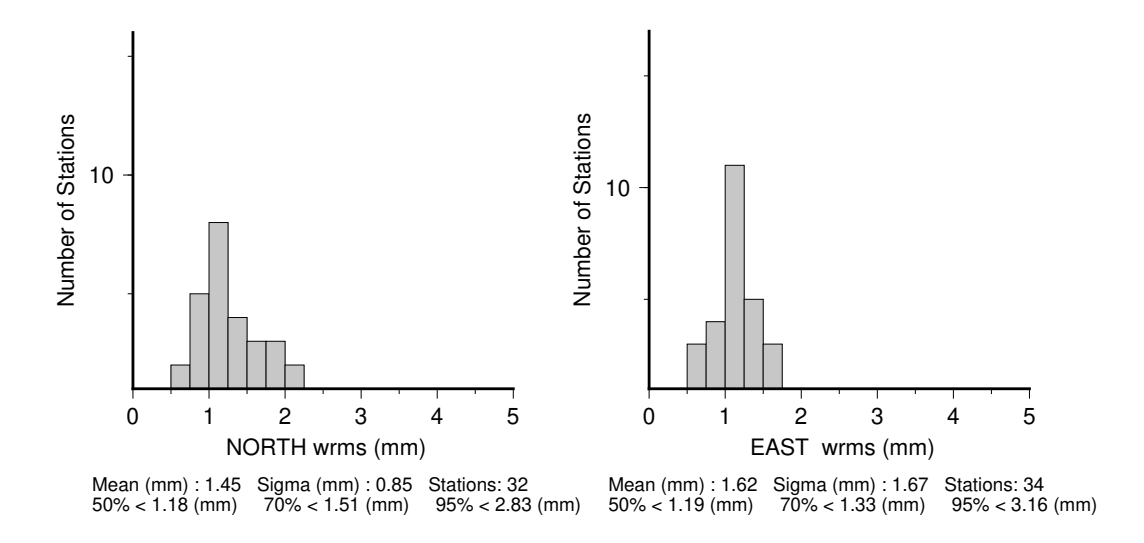
ANET Processing

The ANET additional sites are being processed as a separate network, and the frame-resolved SINEX files will be given in the Antarctica 2007 reference frame (Altamimi *et al.*, 2016, 2017). We label this frame ant14. Time series and SINEX files are generated only for final orbit solutions and are labeled as fanet (instead of final to avoid name conflicts with loose solutions). The IGS14 loose submission files are labeled with "lse14" to differentiate them for the IGS08 loose submissions, which were labeled as loose. The statistics of the time series fits from the CWU solution for this quarter are given in Table 5.

Table 5: Statistics of the fits of 34 stations in the ANET region for CWU analyzed in the final orbit analysis between June 15, 2025 and September 27, 2025.

| CWU | North (mm) | East (mm) | Up (mm) |
|--------|------------|-----------|---------|
| Median | | | |
| ANET | 1.18 | 1.19 | 6.29 |
| 70% | | | |
| ANET | 1.51 | 1.33 | 7.13 |
| 95% | | | |
| ANET | 2.83 | 3.16 | 12.45 |

The histograms of the RMS scatter in NEU of the results for this quarter are shown in Figure A.1



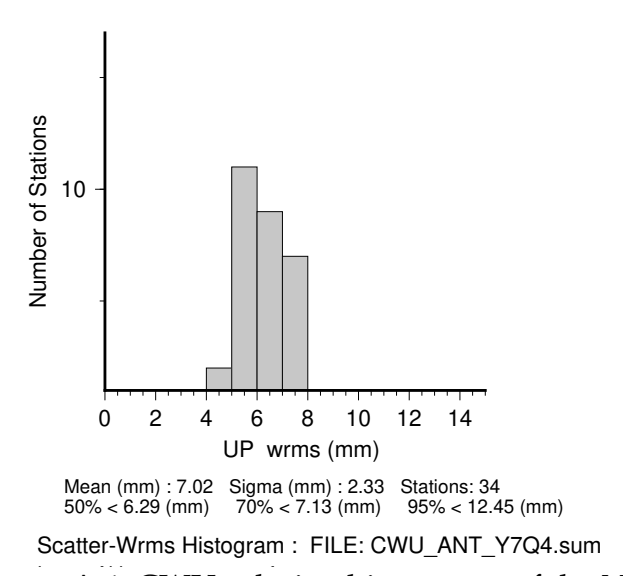


Figure A.1: CWU solution histograms of the North, East and Up RMS scatters of the position residuals for 34 stations in Antarctica analyzed between June 15, 2025 and September 27, 2025. Linear trends and annual signals were estimated from the time series.

References

Altamimi, Z., P. Rebischung, L. Metivier, and X. Collilieux (2016), ITRF2014: A new release of the International Terrestrial Reference Frame modeling nonlinear station motions, *J. Geophys. Res. Solid Earth*, 121, 6109-6131, doi: 10.1002/2016JB013098.

Altamimi, Z., L. Metivier, P. Rebischung, H. Rouby, X. Collilieux; ITRF2014 plate motion model, *Geophysical Journal International, Volume 209*, Issue 3, 1 June 2017, Pages 1906-1912, https://doi.org/10.1093/gji/ggx147